Durability Design With Reliability Methods: A Case Study of Automotive Wheel Assemblies

by

Richard L. Ridder

Project submitted to the Faculty of the
Virginia Polytechnic Institute and State University
in partial fulfillment of the requirements for the degree of

MASTER OF ENGINEERING

in

Engineering Mechanics

APPROVED:

R.W. Landgraf, Chairman

S. Thangjitham

S. L. Hendricks

August, 1992

Blacksburg, Virginia

Durability Design With Reliability Methods: A Case Study of Automotive Wheel Assemblies

by
Richard L. Ridder

Dr. R.W. Landgraf, Chairman
Engineering Science and Mechanics

(ABSTRACT)

The incorporation of reliability theory into a fatigue analysis program is studied. A thorough background in probabilistic methods and metal fatigue is presented, allowing a full understanding of these processes. An automotive wheel assembly is then introduced as an example of the applications of this durability/reliability design package.

A detailed step-by-step procedure is utilized to develop the basic information needed to analyze the wheel assembly: material properties, geometry, and loading; the relationship between applied load and stress; and the degree of variation in specific material properties, wheel thickness, and service loading. An in depth documentation of the effect of these "real world" variations on wheel reliability is then presented in graphical form. Several different approaches in altering the design variables are used in order to thoroughly illustrate the resulting component reliability. Such information is particularly relevant where product quality and warranty formulation are concerned.

ACKNOWLEDGMENTS

The author wishes to acknowledge Professor Landgraf for his insights and contributions to this project. I would also like to express my gratitude to Professor Thangjitham for the use of his subroutine — and for his helpful hints — and to Drs. Hendricks and Heller for serving on my examining committee. In addition, I want to thank graduate students Reza Karkehabadi and Ibrahim Janajreh for their advice and support.

Finally, I would like to convey my sincere appreciation to my parents, Ben and Helen, for their love and support throughout my graduate studies.

Contents

NOTATION

σ . . . . . local stress
ϵ . . . . . local strain
σ_a . . . . . local stress amplitude
ϵ_a . . . . . local strain amplitude
S_a . . . . . nominal stress amplitude
σ_m . . . . . local mean stress
H' . . . . . cyclic strength coefficient (often K')
n' . . . . . cyclic strain hardening exponent
σ'_f . . . . . fatigue strength coefficient
b . . . . . fatigue strength exponent
ϵ'_f . . . . . fatigue ductility coefficient
c . . . . . fatigue ductility exponent
k_f . . . . . fatigue stress concentration factor
N_f . . . . . cycles to failure
$2N_f$ . . . . . reversals to failure
$f_X(x)$ . . . . . probability density function
$F_X(x)$ . . . . cumulative distribution function
$G()$ . . . . . performance function
$R()$ . . . . . strength function
$S()$ . . . . . stress function
$P[\,]$ . . . . . probability of
P_f . . . . . probability of failure
$\phi()$ . . . . . PDF of standard normal distribution
$\Phi()$ . . . . . CDF of standard normal distribution
x_i . . . . . vector of design variables
x_i^* . . . . . iterated value of design variables
β . . . . . safety index
μ_i . . . . . mean value of i-th variable
σ_i . . . . . standard deviation of i-th variable

LIST OF FIGURES

LIST OF TABLES

INTRODUCTION

Design engineers have long known the necessity of accurately predicting the service performance of their components. The fatigue life of a piece of equipment is of prime importance when selecting a material and processing it to perform a specific job, particularly when human safety is involved. However, accurately determining the service life of a component can be quite challenging, due largely to inherent variations in material properties and loading histories. Solving this more realistic problem requires assessment of these variable parameters via probability theory. While this is not a new idea, recent advances in reliability techniques have made fatigue life programs much more valuable to designers, giving them improved qualitative information about actual component performance. The automotive industry is particularly suited for employing such a durability/reliability design package, due mainly to the "unpredictable" nature of product usage. A migration away from strictly deterministic calculations may also be particularly relevant to engineers making quality assurance and warranty decisions. What follows is an introduction to current fatigue analysis techniques, and an in-depth discussion of modern reliability methods. These topics are then synthesized in a case study of automotive wheel assemblies, to clearly illustrate the benefits of such a package to design and quality assurance engineers.

BASIC CONCEPTS

Fatigue Life

For nearly a century, the accepted practice for determining the fatigue life of materials under loading has been the stress-life (S-N) approach. This method is fairly accurate, provided the stress remains in the elastic range, and the measured material life is relatively long (say, over 10^4 cycles). Various parameters could then be added to the S-N equation to account for mean stress effects, notches, surface finish, environmental conditions, loading method, etc. The problem with the S-N approach lies in its failure to consider local plastic deformations that occur in highly stressed notched members; these regions of localized yielding are responsible for specimen damage.

A much better method for predicting fatigue life involves analyzing the localized plastic strains that develop at stress raisers. This strain-life, or ϵ-N, approach uses the stresses and strains in these critical regions to obtain a life estimate. Initial development of a strain–life relation considers once again the relationship between stress and fatigue life — local stress amplitude, σ_a, is plotted against reversals to failure, $2N_f$, on a log–log scale, and a straight line results:

$$\sigma_a = \sigma_f'(2N_f)^b \tag{1.1}$$

Using a power-hardening stress-strain curve such as that of the Ramberg-Osgood type shown in Figure 1 [7, see Chapter 12], the strain amplitude, ϵ_a, can be related to stress amplitude. Substituting the stress amplitude from above into this equation yields the following ϵ-N relation:

$$\epsilon_a = \frac{\sigma_f'}{E}(2N_f)^b + \epsilon_f'(2N_f)^c \tag{1.2}$$

which is a summation of the elastic and plastic strain components as illustrated in Figure 2. The fatigue strength and ductility coefficients (σ_f' and ϵ_f') and their corresponding exponents (b and c) are determined from this figure; as can be seen, material fatigue life is governed by the elastic line at long

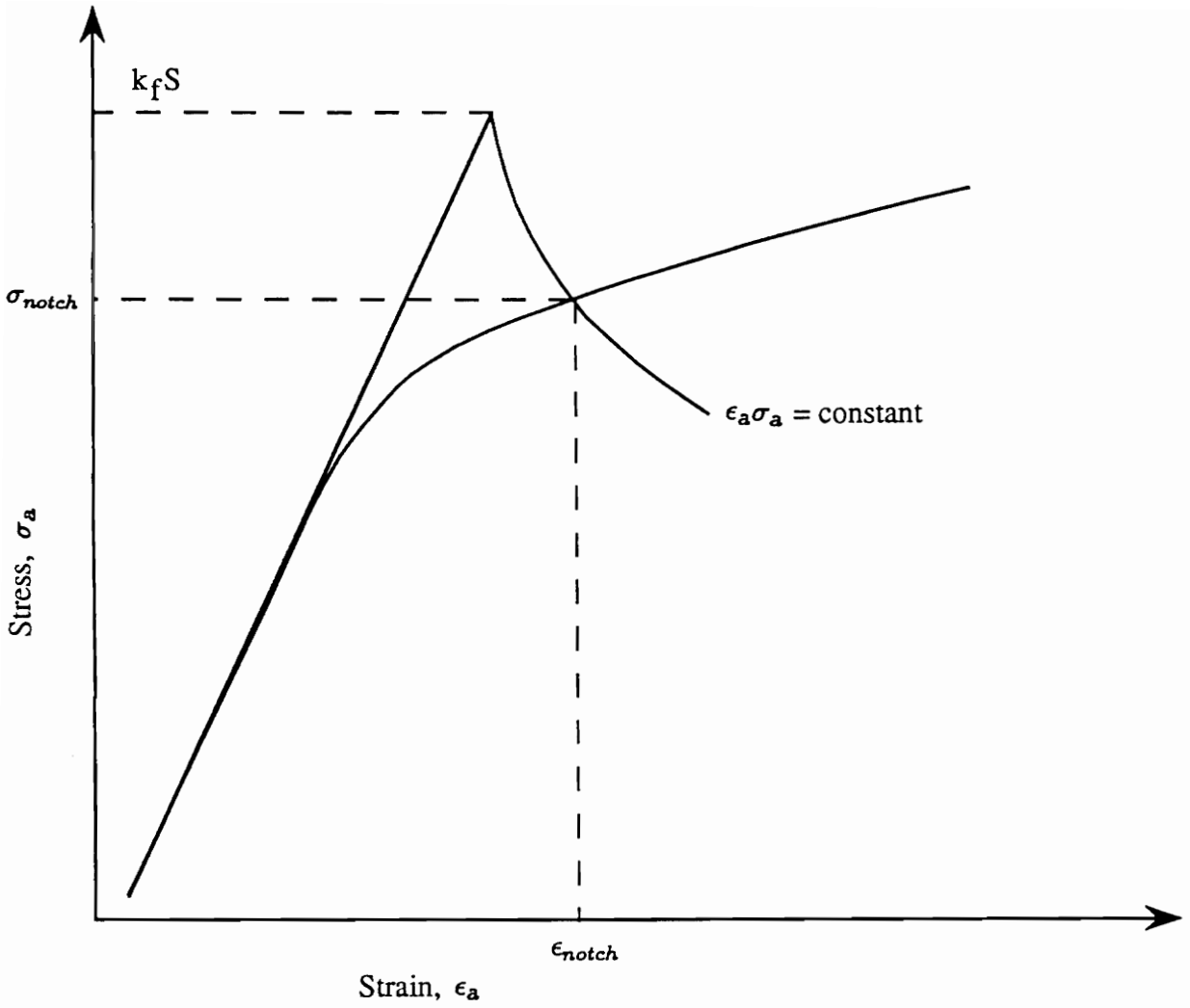

Figure 1 : Ramberg-Osgood stress-strain curve showing intersecting hyperbola

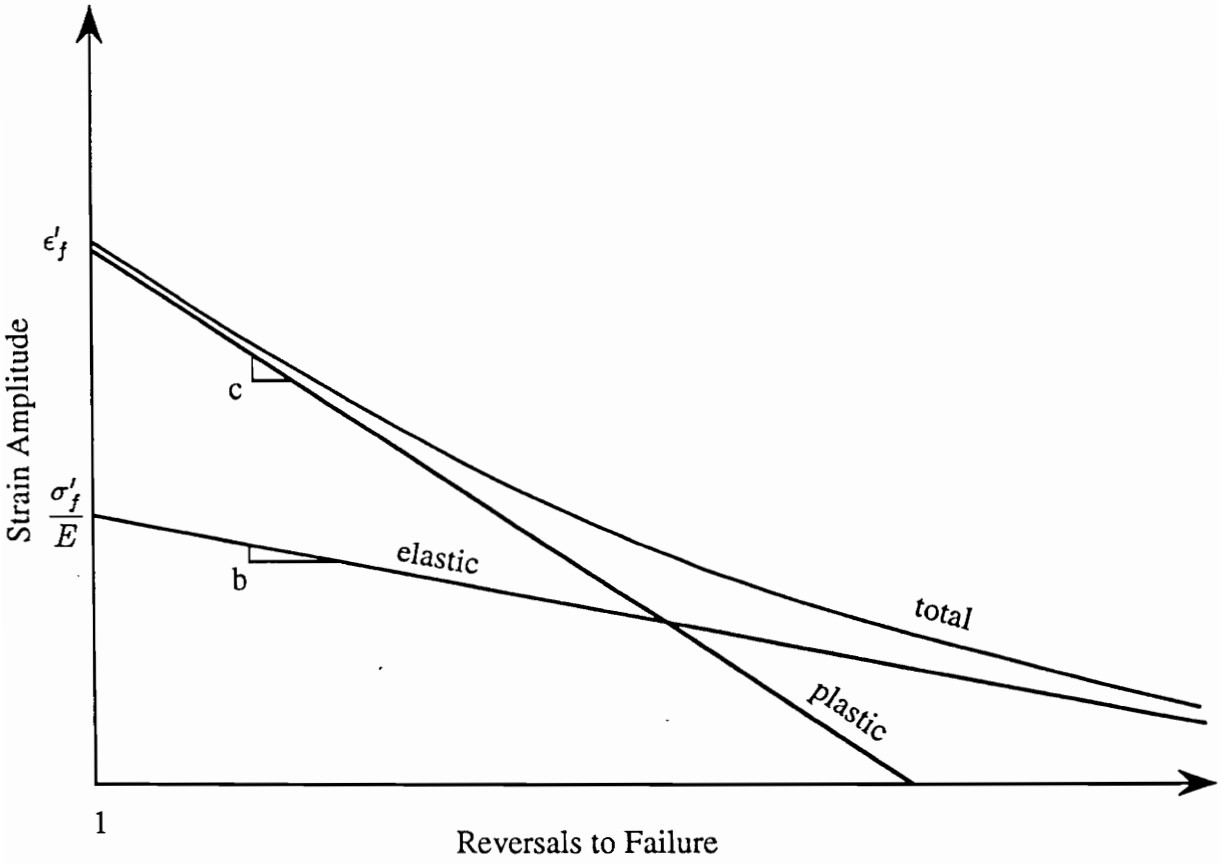

Figure 2 : Strain-Life curve showing material constants

lives, and at short lives by plastic strains. Failure in strain-life analysis is defined as the number of cycles required to cause crack initiation (the smallest detectable crack), not actual specimen failure. A complete life prediction program would include this strain-life analysis and an additional fatigue crack growth algorithm to handle crack propagation to actual specimen failure [9].

Considering the stress that causes plastic deformation at a notch, it is possible to quantify notch stresses and strains in terms of the nominal applied stress, S, and the stress concentration factor, k_f. Assuming nominally elastic behavior, Topper modified an earlier equation developed by Neuber and showed that

$$\sigma_a \epsilon_a = \frac{(k_f S_a)^2}{E} = constant \tag{1.3}$$

for cyclic loading, where S_a is the net section stress amplitude. Plotting σ_a versus ϵ_a gives the equation of a hyperbola (see Figure 1). The point at which this hyperbola intersects the cyclic stress-strain curve gives a good approximation to the actual stress and strain at the notch arising from the applied nominal stress, S.

For completely reversed loading (no mean stress), Smith, Watson, and Topper formulated the following relation by combining Eqs. (1.1) and (1.2) [3]:

$$\sigma_a \epsilon_a = \frac{(\sigma_f')^2}{E}(2N_f)^{2b} + \sigma_f' \epsilon_f' (2N_f)^{b+c} \tag{1.4}$$

which is an all-important fatigue life relationship. Due to the cycle-by-cycle nature of damage accumulation in ϵ-N fatigue, an algorithm is often needed to reduce complex stress histories into a more useful format. Several such routines are available; a common procedure used is rainflow cycle counting, which is detailed in [3].

In summary, a method has been developed to relate material strain to a corresponding fatigue life through knowledge of local stresses and strains. By taking local plasticity effects into account, a much more representative fatigue life can be established. These equations will be used in formulating a relationship between material strength and fatigue life in later discussions.

Probability Theory

Classical probability theory utilizes statistical distributions of variables in the form of probability density functions. These functions of random variables in essence describe events numerically, so that the probability of an event occurring can be easily determined. For example, if $f_X(x)$ is the probability density function of X, then the probability of X being in the interval $(a,b]$ is defined as

$$P(a < X \leq b) = \int_a^b f_X(x)dx \tag{1.5}$$

provided f is continuous.

Two quantities commonly used to describe a random variable are the *mean* and the *variance*. The mean, or expected value of a random variable is written as

$$E(x) = \int_{-\infty}^{\infty} x \cdot f_X(x)dx = \mu_X \tag{1.6}$$

and is characterized as being the centroid of the area under the distribution curve. The variance of a random variable measures the dispersion of values about the mean value:

$$Var(x) = \int_{-\infty}^{\infty} (x - \mu_X)^2 \cdot f_X(x)dx = \int_{-\infty}^{\infty} x^2 \cdot f_X(x)dx - \mu_X^2 \tag{1.7}$$

The *standard deviation,* then, is simply the square root of the variance. Physically, the standard deviation is the radius of gyration of the normalized area about its centroid [1].

For the case of multiple random variables, a *joint probability density function* is developed to express all of the distributions in terms of their individual probabilities of occurrence:

$$\begin{aligned} &\int_a^b \int_c^d \cdots \int_y^z f_{X_1,X_2,\ldots X_n}(x_1, x_2, \ldots x_n)dx_1 dx_2 \ldots dx_n \\ &\quad = P[(a < X_1 \leq b) \bigcap (c < X_2 \leq d) \bigcap \ldots (y < X_n \leq z)] \end{aligned} \tag{1.8}$$

Because each random variable represents an event with a corresponding probability of occurrence, more often than not these events affect one another, and the variables are said to be correlated. If independence of random variables is assumed, however, the mean and variance can be computed in a fashion similar to that just described [12]. These properties will be employed as the primary descriptors of random variable distributions in the ensuing section.

Engineering Reliability

Failure of a component can be stated as the condition arising when the component can no longer perform the specific function for which it was intended. In mathematical terms, a failure is denoted by the stress S exceeding the strength R, or by the equation $R - S < 0$. If these values are deterministic in nature, the failure state is easily identified and avoided. However, if the strength and stress depend on several other variables, such as processing, geometry, and load variations (which is almost always the case), then the values R and S will themselves vary, and the failure state can no longer be avoided by simply keeping the accepted value of S less than that of R. If the stress and strength can be modeled as Gaussian (normal) distributions, an overlap will exist between the curves where failure may occur due to the possibility of R being less than S. Figure 3 shows this region of "unreliability," as it is sometimes called [13].

Often the design variables are expressed in terms of a single *performance function*, *G(R,S)*. A *limit-state equation* is then defined which separates the states of survival and failure:

$$G(R, S) = G(X_1, X_2, \ldots X_n) = 0 \tag{1.9}$$

In terms of all the design variables X_i, then, the probability of failure P_f may be defined as

$$P_f = \int \int \ldots \int f_{X_1, X_2, \ldots X_n}(x_1, x_2, \ldots x_n) dx_1 dx_2 \ldots dx_n \tag{1.10}$$

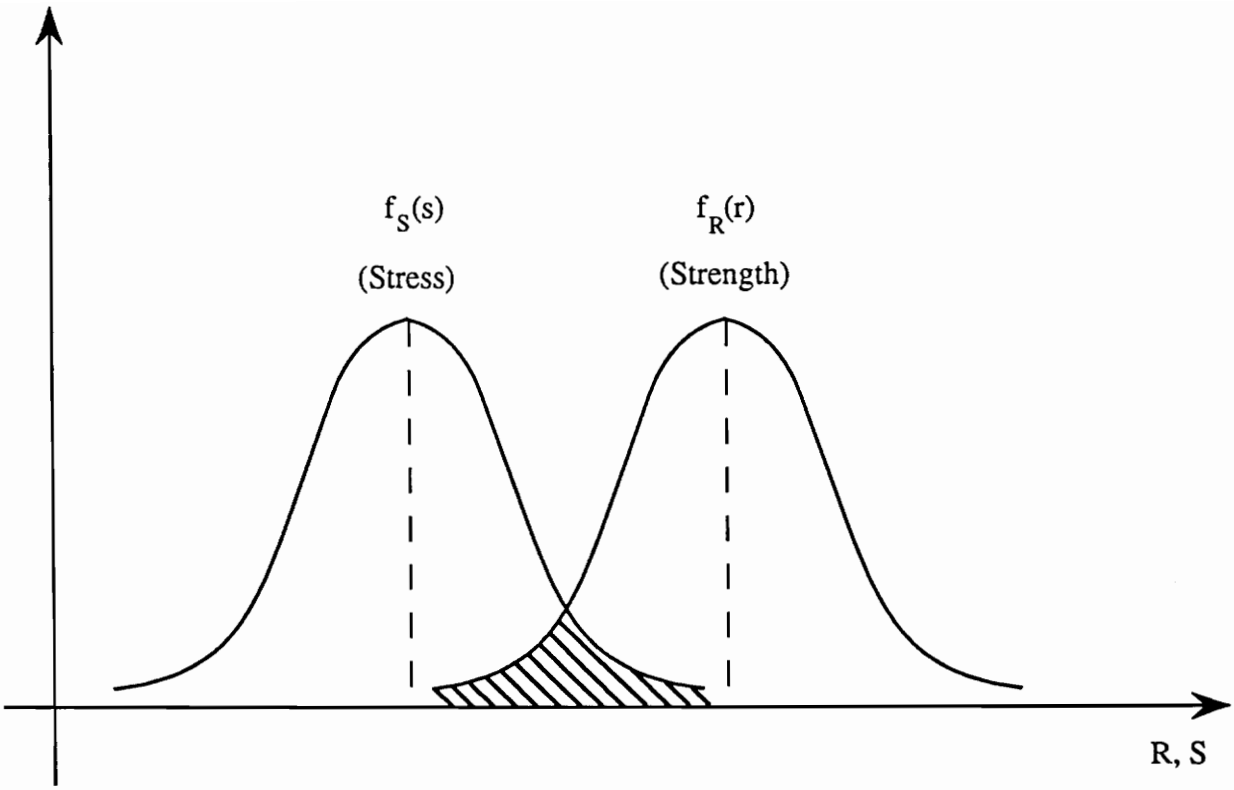

Figure 3 : Region of R-S Interference (unreliability)

where $f_{X_1,X_2,\ldots X_n}$ is the joint probability density function of the design variables $X_1, X_2, \ldots X_n$ and the integration is performed over the region where $G < 0$ (failure state). In many cases the data will be insufficient to determine the joint probability function, and multiple integration over the design variables can prove quite cumbersome. For this reason other methods to determine the probability of failure are utilized. A relatively modern procedure involves the first two moments of the design variables, the mean and the variance. The *first-order second moment*, or *FOSM*, method expresses the system P_f in terms of a safety index, β. In a two-dimensional reduced variate plot of stress vs. strength, the safety index represents the coordinates of the most probable failure point on the $G = 0$ line, the boundary separating states of survival and failure (for multi-dimensional cases, $G = 0$ actually defines a surface). This *design point* is the point lying closest to the origin, and for linear G is obtained by simple geometry [2] (see Figure 4):

$$\beta = \frac{\mu_R - \mu_S}{\sqrt{\sigma_R^2 + \sigma_S^2}} \tag{1.11}$$

where $\mu_{R,S}$ and $\sigma_{R,S}$ are the means and standard deviations of R and S, respectively. For normally distributed R and S, the probability of failure is then ascertained using tables of the Standard Normal Distribution Function, $\Phi(\cdot)$:

$$P_f = 1 - \Phi(\beta) \tag{1.12}$$

If the performance function $G(R,S)$ is nonlinear, however, iteration is needed to reach the design point. This process is detailed in Figure 5. Values of the iterated normal variables X_i^* are obtained through the relation

$$X_{i(j)}^* = \mu_i + \alpha_i \beta_j \sigma_i \tag{1.13}$$

where β_j is the safety index corresponding to the j-th iteration, and

$$\alpha_i = \frac{-\frac{\partial G}{\partial X_i}\sigma_{X_i}}{\sqrt{\sum_i (\frac{\partial G}{\partial X_i}\sigma_{X_i})^2}} \tag{1.14}$$

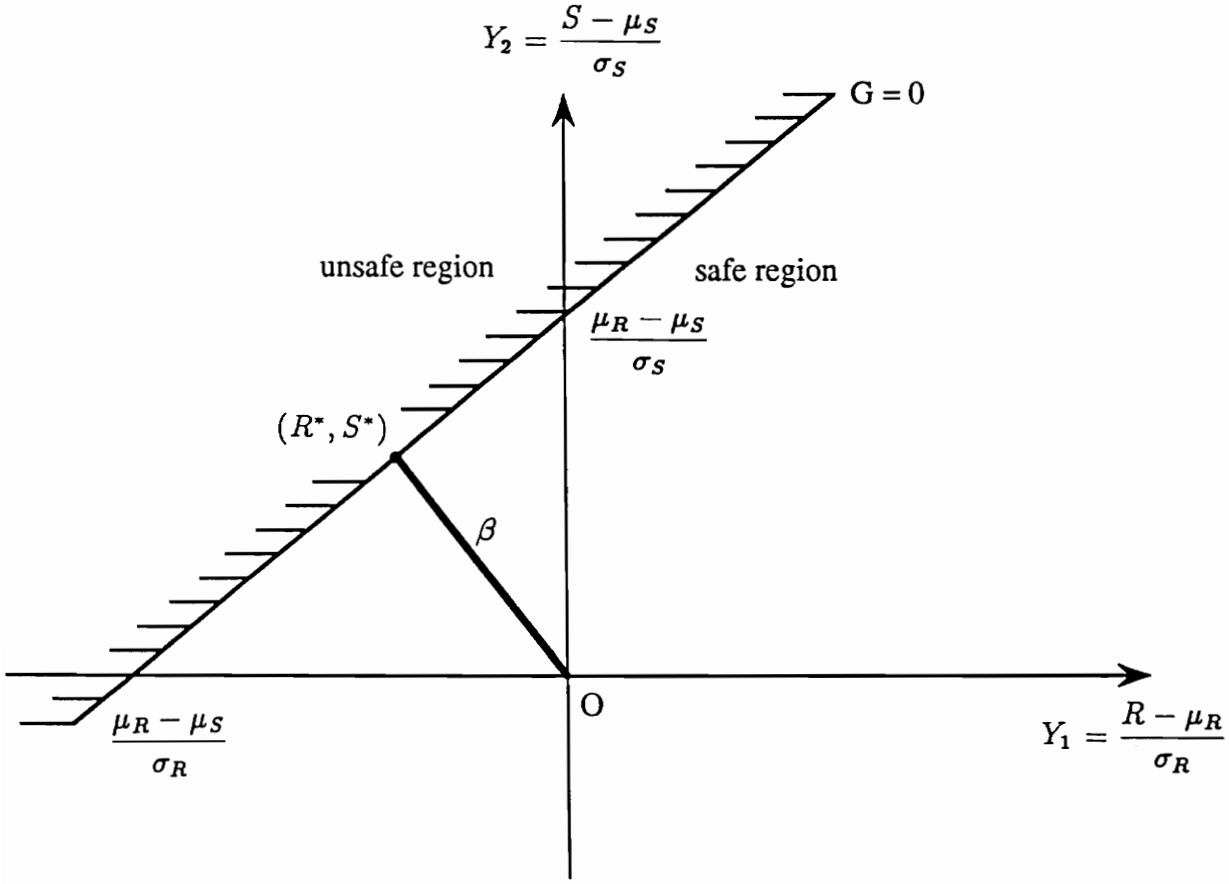

$$\beta = \frac{\mu_R - \mu_S}{\sqrt{\sigma_R^2 + \sigma_S^2}}$$

Figure 4 : Safety Index and Most Probable Failure Point for linear G

is evaluated at the most recent design point. Iteration usually begins at the mean value of each variable. Since β is initially unknown, Eq. (1.13) is substituted into the limit-state equation (1.9) and the resulting equation is solved for β_j. This value is then used in Eq. (1.13) and the first iterated values for the design point ($X_{i_1}^*$) are obtained. The process continues until the values of X_i^* and β_j stabilize. The P_f is then evaluated as per Eq. (1.12), and the last values of X_i^* represent the most probable failure point of the system. Refer to the flow chart in Figure 5 for additional clarification.

Random variables need not be normally distributed; when dealing with other distributions, an equivalent normal transformation must be performed in order to express the means and standard deviations in terms of a normal distribution:

$$\mu_{X_i}^N = X_i^* - \sigma_{X_i}^N \Phi^{-1}[F_{X_i}(x_i^*)] \tag{1.15}$$

$$\sigma_{X_i}^N = \frac{\phi\{\Phi^{-1}[F_{X_i}(x_i^*)]\}}{f_{X_i}(x_i^*)} \tag{1.16}$$

The means and standard deviations of each variable will then change with each iteration. This is the so-called Advanced Format FOSM technique. Since the FOSM method described here assumes independence of design variables, a case involving correlated variables requires an additional orthogonal transformation [2].

The First-Order Second Moment method is a powerful tool for evaluating component reliability when parameters such as loads, geometry, processing, and environmental effects cannot be represented deterministically. Even though qualitative information about the distribution of each variable is needed, accurate results can still be achieved by making reasonable assumptions when necessary. If little data is available on a particular variable, a high dispersion could be assumed, which will yield a slightly conservative (lower) value for the system reliability, depending on the significance of the variable. Obviously, care should be used in making such assumptions.

With a background in both metal fatigue and reliability in hand, it is now

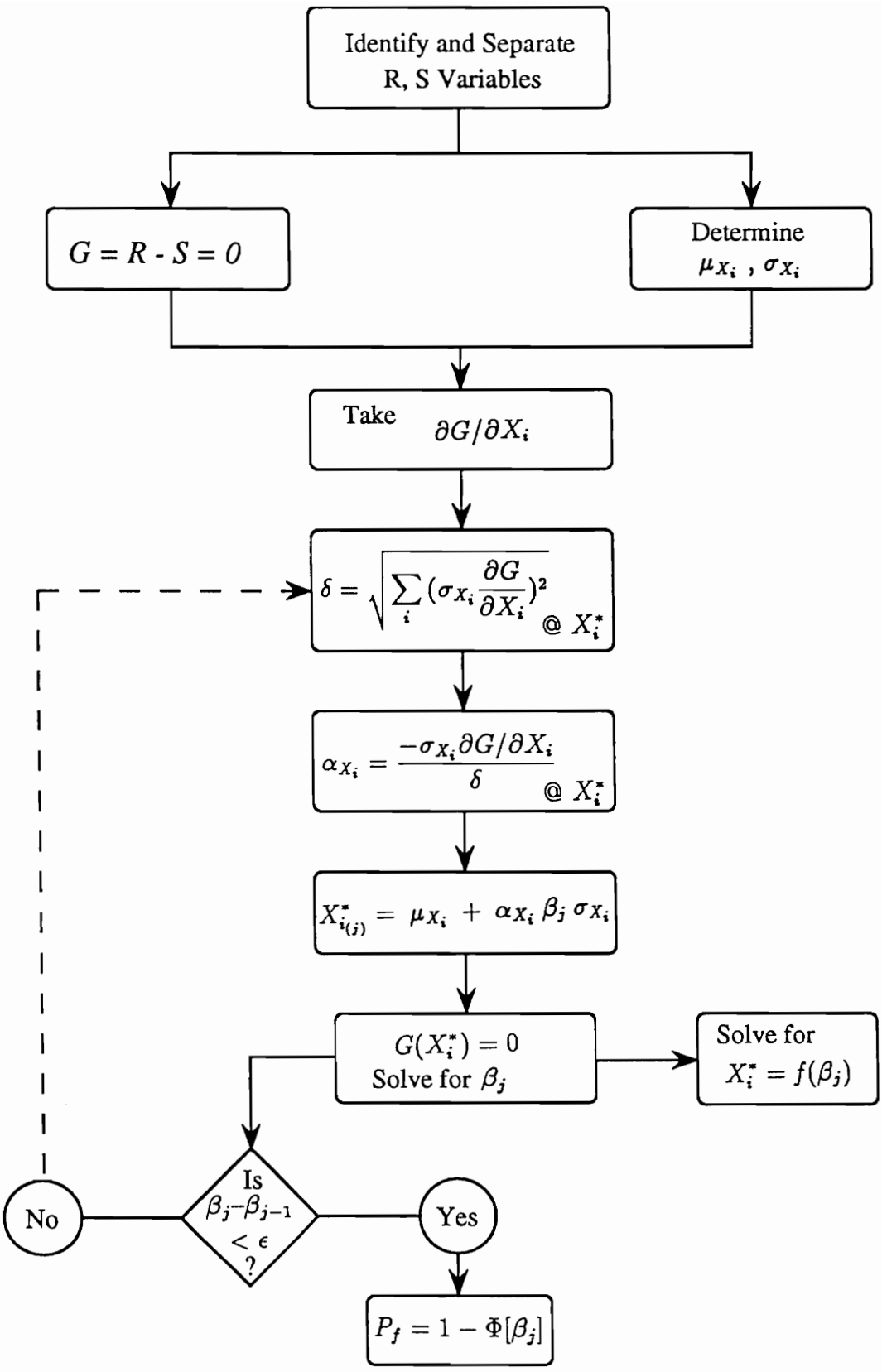

Figure 5: Design point iteration scheme for normal variables

possible to proceed with this information and apply it directly to a real-world problem. The following case study illustrates the benefits of synthesizing these topics into a practical engineering tool — one that may be modified as necessary to solve numerous types of problems.

THE AUTOMOTIVE WHEEL REVISITED

Introduction To Case Study

Automotive design engineers are challenged by a number of problems in the modern industrial environment. Economics dictate the need to develop more efficient and durable products in a cheaper and more expeditious manner than ever before. To accomplish this monumental task, several analytical tools are currently available to assist the designer: laboratory computer simulation of vehicle kinematics and service loads, which reduce the need for lengthy proving ground tests; finite element software that accurately analyzes component stresses; and fatigue damage programs which can predict component performance. These tools can minimize the design/development time of a component or structure considerably by predicting its performance before it enters production, thus allowing designers to tackle unforeseen problems early on and accelerate subsequent design improvements.

Automobiles are designed with mass-production and cost-effectiveness in mind; consequently, engineers have to take into consideration the non-redundant structure of the vehicle, its wide variation of service loading possibilities, and a usage history void of periodic safety inspections when designing every strategic component of the vehicle. Obviously, here it is crucial to be able to predict as accurately and thoroughly as possible a component's performance while still in the design/development stage. This case study illustrates the synthesis of reliability and fatigue life algorithms into a program to estimate the performance of a wheel spider over a wide variety of service routes and driver spectra.

Much work has already gone into designing and improving automotive wheel assemblies in efforts to reduce weight and increase durability (the wheel is an unsprung mass, and as such should be kept as light as possible). It has been noted that fully 98% of wheel spider (disc) damage results from bending moments induced during cornering maneuvers [14]; as a result, braking and acceleration effects can be ignored. These bending moments are a function of vehicle weight, geometry, and lateral acceleration, though, and driving habits and terrain will greatly influence wheel spider damage. It is for this reason that a method is needed to analyze these driver and road variabilities — as well as the variations in material properties and geometry — in order to better quantify the resulting wheel damage. A significant part of any analysis procedure involves presenting the results in a useful format; to this end, several different approaches will be taken in displaying the information, so that a thorough knowledge of the component's service performance may be acquired.

The basic steps involved in durability/reliability design are outlined in Figure 6. It is assumed initially that the material properties, geometry, and applied loads are either known or easily accessible, although no distributions of these values are needed as of yet. The process is then divided into stress and strength elements, which may require detailed computation (all steps are examined in-depth in the following section). It is at this point that an ordinary fatigue-life or damage algorithm would employ a damage parameter and a cumulative damage rule in order to calculate a service life from the above deterministic properties [8]. However, with information regarding the distribution of these values, a probabilistic approach may be used to better predict component performance and life. This method is unequivocally more attuned to "real world" situations, as no part or property can be *exactly* reproduced by current methods. In addition to the distributions, data regarding physical and personal driving variations and material processing effects are incorporated in various forms into the calculations of R and S.

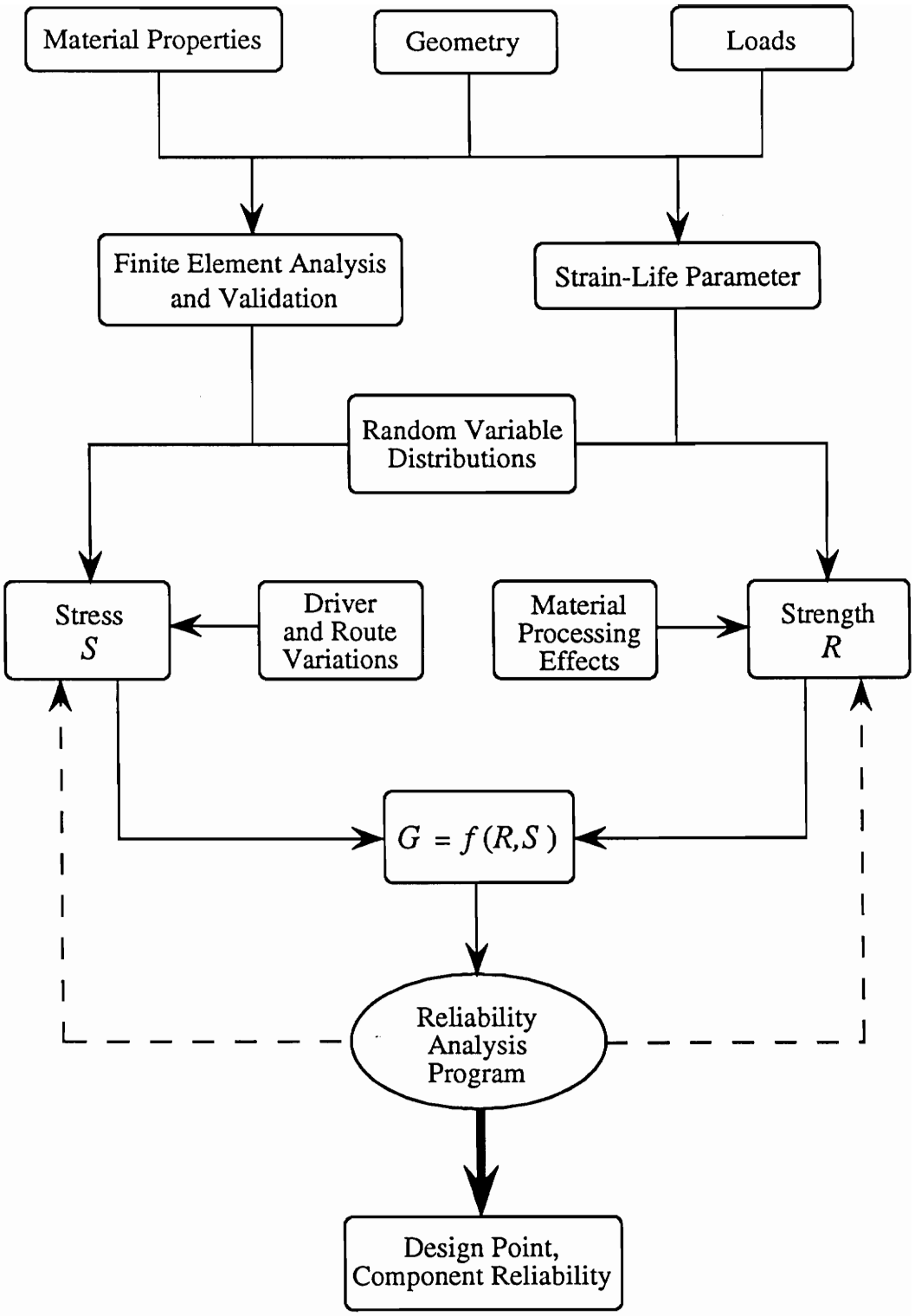

Figure 6: Flow Chart for Durability/Reliability Analysis

These stress and strength functions are then combined into the performance function, *G(R,S)*. This function is called repeatedly by the reliability analysis program, which uses an iterative scheme described in the Engineering Reliability section (due to the extent of the iterative process, a separate flow chart was shown in Figure 5). Once iteration is complete, the probability of failure and the design point are given. The reliability of the component is portrayed in terms of its probability of failure, where

$$Reliability = 1 - P_f \tag{2.1}$$

Thus, the reliability will always be identified as a number between zero and one.

Each step of this fatigue/reliability procedure will now be explained in further detail.

Properties, Geometry, and Loading

Material properties are well-documented and researched, but while extensive amounts of data are available, no single large database of such information exists outside of corporate boundaries. The cyclic properties utilized in this case study were acquired from Ford Motor Company's database of material properties [6] and from work done by their research staff involving material processing (cold working) effects. For this case study, three representative materials were chosen for analysis, based mainly on their diversity of properties, and previous application in this area: SAE 1010 hot-rolled, low-carbon (HRLC) steel, DP80T dual phase high-strength, low-alloy (HSLA) steel, and 5454 aluminum. The data for these alloys are summarized in Table 1.

Knowledge of the specimen geometry consisted of thickness measurements of a 14×5-inch wheel spider incremented in the radial direction (a finite element mesh of this component is shown in Figure 7). This thickness data for both steels is represented by a mean and standard deviation value in Table 1.

Table 1: Cyclic Material Properties and Distributions

Metal	*thickness* (inches)	E (ksi)	σ_f' (ksi)	b	ϵ_f'	c
SAE 1010 (σ)	0.1469 (0.0045)	29,500 (59.0)	88.5 (8.85)	-0.096	0.16 (0.024)	-0.44
20% CW (σ)			76.5 (7.65)	-0.065	0.17 (0.026)	-0.45
Dual Phase (σ)	0.1112 (0.0039)	30,000 (60.0)	174.6 (17.46)	-0.0868	0.3148 (0.0472)	-0.5856
20% CW (σ)			174.6 (17.46)	-0.062	0.3148 (0.0472)	-0.5856
5454 Al (σ)	0.225 (0.0067)	10,000 (20.0)	82.0 (8.20)	-0.116	1.78 (0.267)	-0.85
20% CW (σ)			82.0 (8.20)	-0.103	1.75 (0.263)	-0.80
Std. Deviations σ (% of mean)	~3%	0.2%	10.0%	none	15.0%	none

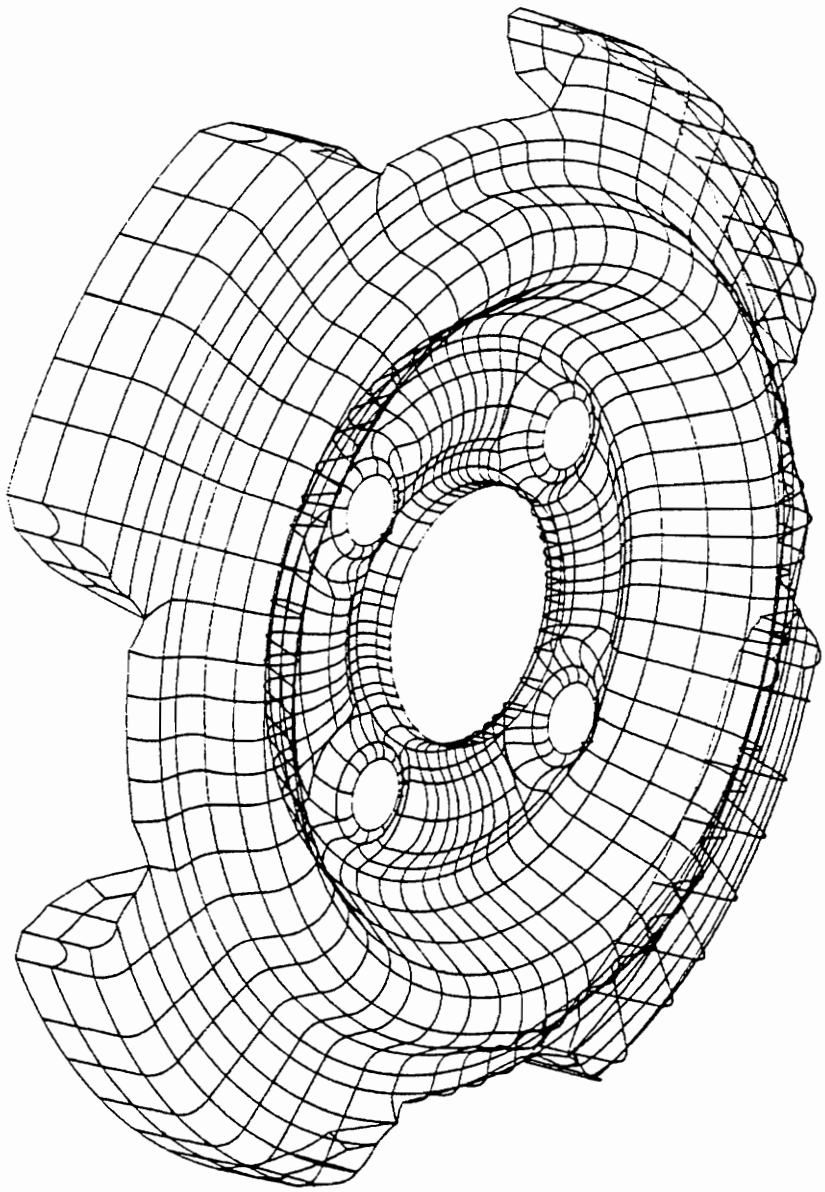

Figure 7: Mesh of the Wheel Spider Shape used in case study

Raw data for the aluminum spider was not available, but a representative thickness was used from information given in [10].

As an initial applied load, various moments were chosen based on the magnitude of the moments used in an SAE constant-amplitude fatigue test (1528 and 1900 ft·lbs). This SAE test involved rotating a wheel assembly at a constant rate and applying a moment to the wheel through a hub-moment arm linkage, thereby simulating a cornering maneuver. As the test progressed, fatigue cracks that developed would allow the moment arm to deviate past a predetermined "failure" point, and the final cycle count would then be taken as the fatigue life of the wheel (SAE standards require 90% of wheels tested – a life factor of B_{10} – to survive 50,000 cycles at 1528 ft·lbs). This test used moments that were a factor of 1.6 higher than the maximum moment developed in an actual vehicle cornering maneuver, to account for impact loadings and the like [11]. Consequently, the initial moments chosen in this case study are also excessive and are better suited for material comparison purposes rather than actual service life prediction.

Stress and Strength Determination

Preliminary computer analysis of the wheel spider consisted of finite element modeling of the stresses induced by a bending moment applied through the hub area. The stresses that developed in several critical areas over one wheel revolution were recorded, and a relationship then drawn between stress range, material thickness, and applied bending moment [9]. As a result of the symmetrical nature of the wheel stresses, the stress amplitudes were completely reversed, and no mean stress effects came into play. Since the finite element analysis used could not account for plasticity effects, local stresses in excess of the material's yield strength were handled by making a plasticity correction of sorts similar to that used for notched members. Specifically, the modified hyperbola of Eq. (1.3) was plotted on the σ-ϵ curve for each material, and the point of intersection used as an approximation to the actual

stress and strain at the critical point.

Results from finite element analysis of the spider were confirmed by the LBF Laboratory in Darmstadt, Germany. Strain gages were employed on a prototype wheel assembly to record the magnitude of strains resulting from an applied bending moment. These strains were then compared to the FEA strains for validation. The relationship between stress range, thickness, and bending moment as derived from the finite element testing is [9]

$$S_a \equiv f(M,t) = K \cdot M \cdot (t^{-1.4}) \tag{2.2}$$

where K is a constant depending on the wheel geometry.

Initial prototype testing consisted of the standard SAE fatigue test previously described. By this method the constant K was ascertained, and the applied stress could now be expressed in terms of a moment and material thickness:

$$S_a = 0.153 \cdot M \cdot (t^{-1.4}) \tag{2.2}$$

with S_a in ksi and M in kip-inches. This is the stress relation that will be used in determining the reliability of the wheel spider.

Formulation of the strength equation required the use of Eq. (1.4):

$$\sigma_a \epsilon_a E = (\sigma_f')^2 (2N_f)^{2b} + \sigma_f' \epsilon_f' E (2N_f)^{b+c} \tag{2.3}$$

By modifying the hyperbola equation,

$$\sigma_a \epsilon_a E = (k_f S_a)^2 = constant \tag{1.3}$$

it becomes evident that the two equations can be combined:

$$(k_f S_a)^2 = \sigma_a \epsilon_a E = (\sigma_f')^2 (2N_f)^{2b} + \sigma_f' \epsilon_f' E (2N_f)^{b+c} \tag{2.4}$$

Due to the plasticity correction that was applied to the finite element results, the combined quantity $k_f S_a$ now represents the true elastic stress amplitude due to the notch effects in the spider. This quantity is renamed S_a^* for

simplicity, but it is important to remember that this does not imply k_f equals unity. In its final form, then, the strength equation R becomes

$$S_a^* = [(\sigma_f')^2(2N_f)^{2b} + \sigma_f'\epsilon_f' E(2N_f)^{b+c}]^{1/2} \tag{2.5}$$

This equation, together with the stress equation (2.2), comprise the performance function used in computing system reliability.

Random Variable Distributions

It is appropriate at this stage to present the primary focus of this case study, which is to introduce real-world variabilities into fatigue-life calculations, in an effort to better predict a component's actual service life. Essentially, the first step of the flow chart shown in Figure 6 involves three categories, each of which is affected by some form of variability. While the loads applied to a wheel assembly may vary due to personal driving habits and terrain (which will be dealt with later), the variations in material properties and geometry are inherent as a result of mass-production techniques. In an attempt to assimilate these variabilities, several cyclic material properties have been "assigned" dispersions representative of industry's ability to control them. Specifically, Young's modulus and the fatigue strength and ductility coefficients were chosen as random variables for each material. These variables, characterized by a mean and standard deviation, are given in Table 1. Values acquired from data tables and other sources were taken as the mean of each random variable; the rationale behind assigning a value to the standard deviation lies in the ability of a manufacturer to reproduce its products' material properties. The modulus of elasticity, for example, is very well defined; this σ-ϵ slope is determined very accurately by modern computational methods. Notwithstanding, the modulus was still chosen as a random variable because of its magnitude in comparison with the other variables and constants in the performance function – it was given a very small standard deviation of 0.2% of the mean value. As for the fatigue strength

and ductility coefficients, which are not nearly as precisely controlled, a larger representative dispersion was needed, based on work done by Boardman [5]. For this case study, values of 10 and 15% (of μ), respectively, were chosen as good estimates of a standard deviation for σ'_f and ϵ'_f.

The fourth random variable required no variance assumptions, as thickness data measured from formed steel wheel spiders was available. This data was entered into a spreadsheet program, which automatically calculated the mean and standard deviation for a normal distribution. In comparison with the material property dispersions, the thickness values for both steels had deviations of about 3% of the mean. The assumption here (at least initially) was that the thickness data resembled a normal distribution. A later portion of the case study involves choosing different distributions for all random variables, in an attempt to better model their actual distributions. If specific data on distributions is not available (as was the case for all three of these variables), careful approximations based on completed work and practical engineering judgment can often provide a quite adequate substitute and qualitative results.

Reliability Program

The integral part of this whole operation is the reliability program itself, which utilizes all the material properties, geometry, loads, stresses and strengths, and distributions in computing a probability of failure at a given cycle count, or service life. Source code for a fundamental program is given in the Appendix. What follows is an abbreviated explanation of the program procedures.

After the initialization steps, deterministic values of the fatigue strength and ductility exponents (in this case for SAE 1010 steel) are entered and manipulated according to the strength equation (2.5) to minimize computing time. Properties of the random variables are then entered and vectors of applied moments and cycle counts are computed. The essential reliability

analysis takes place inside the nested loop at line 40. In the outer loop, the common variable *RMOMT* is given a value from the vector *AMOMT()*. The inner loop assigns the other common variable *RLIFE* a value of twice the cycle number stored in *RCYCL()* (converting from cycles to reversals). The continuation line of both loops is a call to the subroutine *FNBETA()*.

This subroutine is the work of Dr. Surot Thangjitham. Essentially, the subprogram takes all of the information given regarding the random variable distributions and the performance function *G(R,S)* and undergoes an iterative process similar to that shown in Figure 5. The subroutine makes several calls to the function *GFNTN()*, and values of the random variables stored in *VECT()* change slightly with each call — thus changing the value of *G* — until the design point is reached (recall that iteration begins at the mean value of each variable). A probability of failure is then calculated as per Eq. (1.13) corresponding to the applied moment and the given cycle count. The process is repeated for each incremented cycle count in the inner loop of the main program, yielding a failure versus cycles curve for each applied moment. This was the algorithm actually used as an initial analysis of the wheel spider; future program changes will be explained as the more detailed procedures are introduced.

All of the information needed to analyze the wheel is now present, and a comprehensive investigation of its performance and estimated service life can be undertaken. Following are several different analytical tests carried out on the wheel assembly, which will illustrate the effect geometry and loading variations have on the component's fatigue life.

WHEEL ANALYSIS AND LIFE PREDICTION

SAE Standard Test

Initial analysis of wheel spider performance took the form of a constant-amplitude bending moment test similar to the SAE fatigue test. Utilizing the predescribed reliability program, failure vs. cycles curves were developed for each alloy by incrementing the applied moments in a programmed loop. These applied moment values chosen were based on the 1528- and 1900 ft·lb standard SAE fatigue test; moments between 12 and 20 kip·inch were used to approximate the magnitudes of the SAE test, and at the same time give some idea of the wheel's performance if the scaling factor of 1.6 is disregarded (note that 1528 ft·lb = 18.34 kip·in, and $18.34/1.6 \approx 12$ kip·in). The results of this test are shown in Figure 8.

As can be seen by the curves, the dual phase steel fared the best of the three alloys, with a markedly lower probability of failure at equivalent cycles. On the other hand, the SAE 1010 steel had the most rapid increase in P_f, with a fatigue life more than an order of magnitude less than that of the dual phase. The aluminum wheel, while having a shallower curve, offered minimal improvement in reliability over the 1010 — at 10^6 cycles and 12 kip·in, the P_f was seen to be $\sim$0.4 compared to $\sim$0.7 for 1010 steel. For comparison purposes, Recall that SAE standards require 90% of wheels loaded to 1528 ft·lbs to survive a minimum of 50,000 cycles. The 18 kip·inch curve (approximately 1528 ft·lbs) for each material is shown to yield a failure probability between 0.08 for dual phase and 0.5 for aluminum at 50,000 cycles. So, the detrimental effects of material property and thickness variations (as well as under-design) can already be seen in the HRLC and aluminum wheel assemblies.

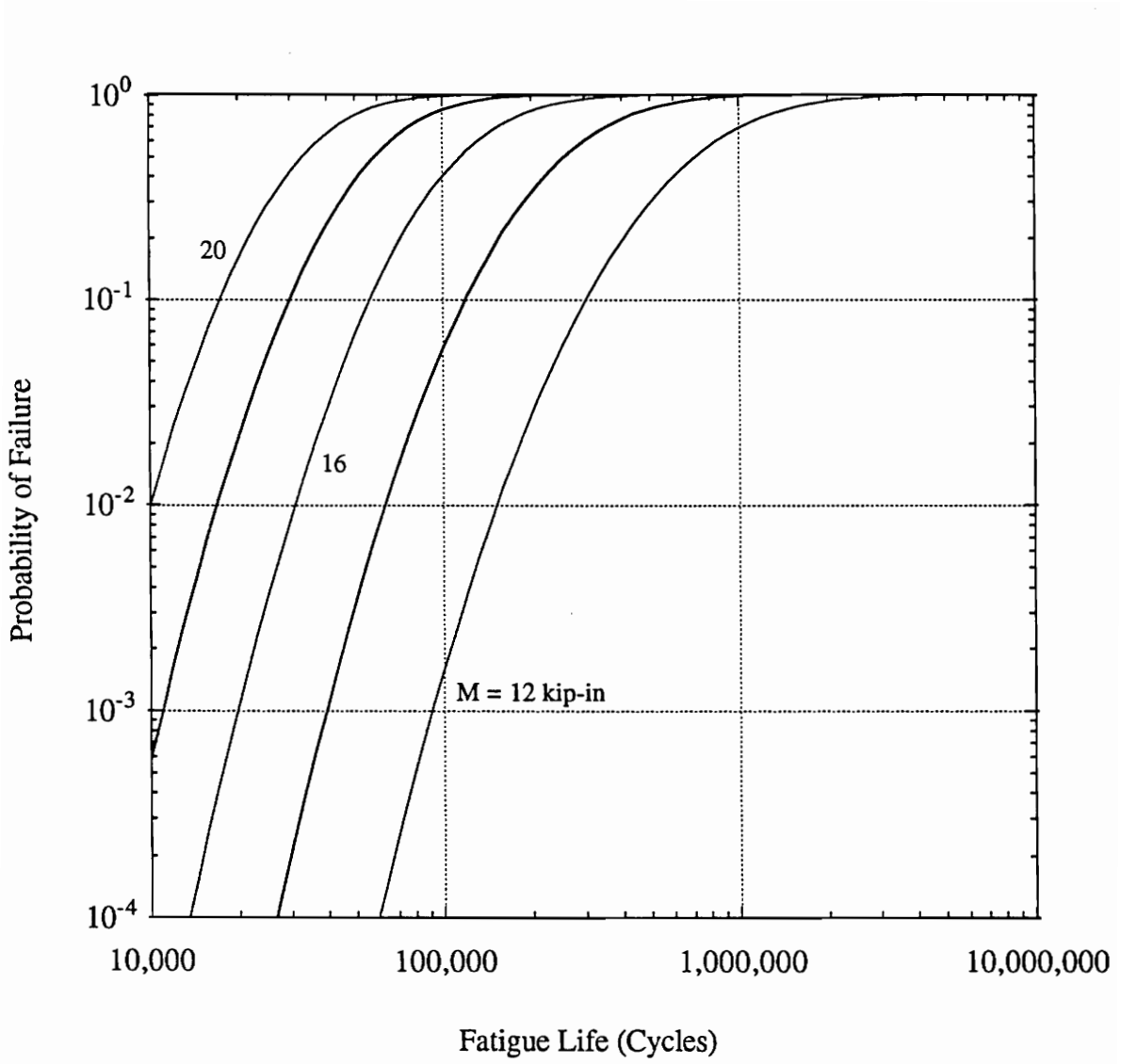

Figure 8a : P_f vs. Cycles for SAE 1010 Steel

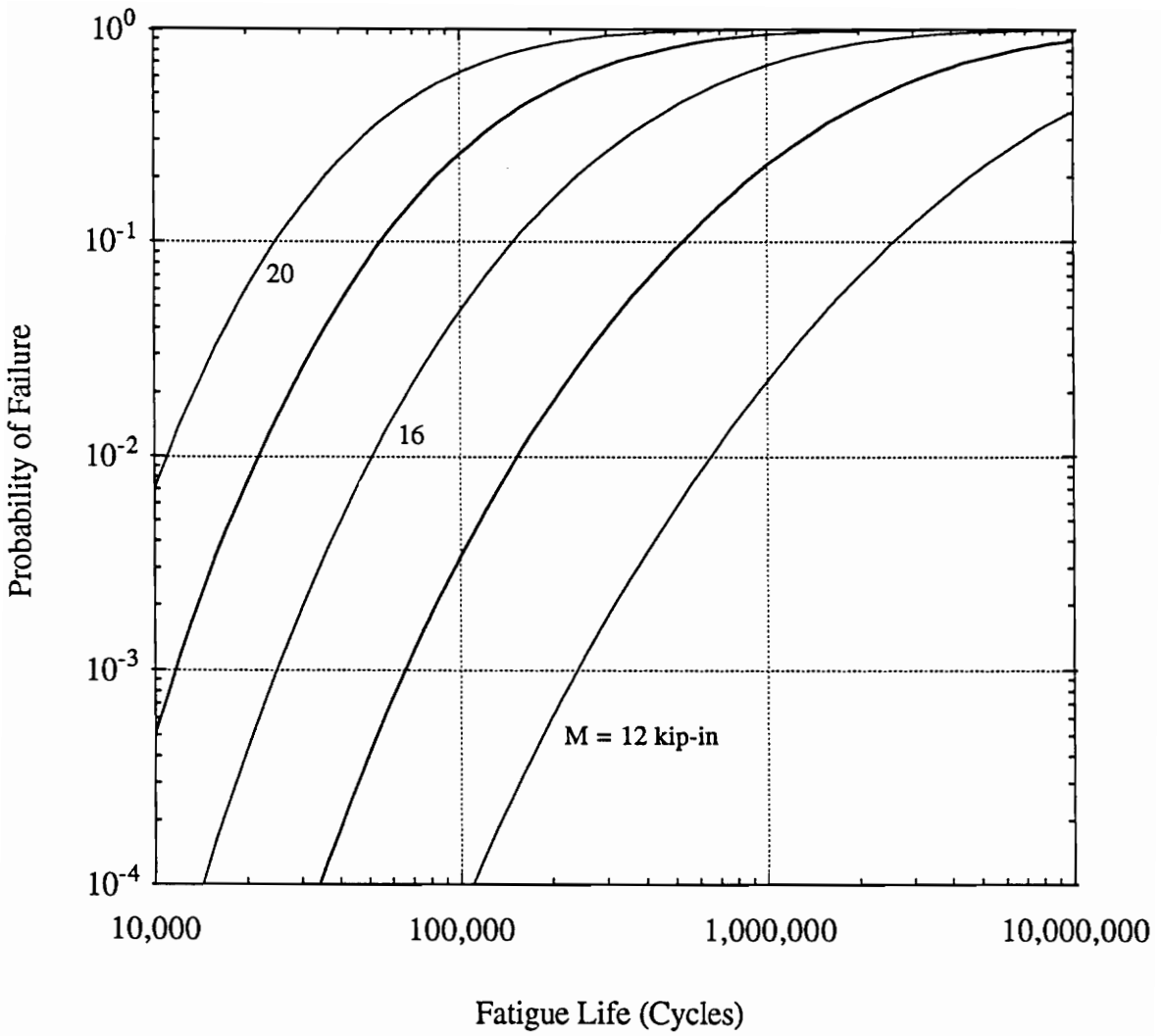

Figure 8b : P_f vs. Cycles for Dual Phase Steel

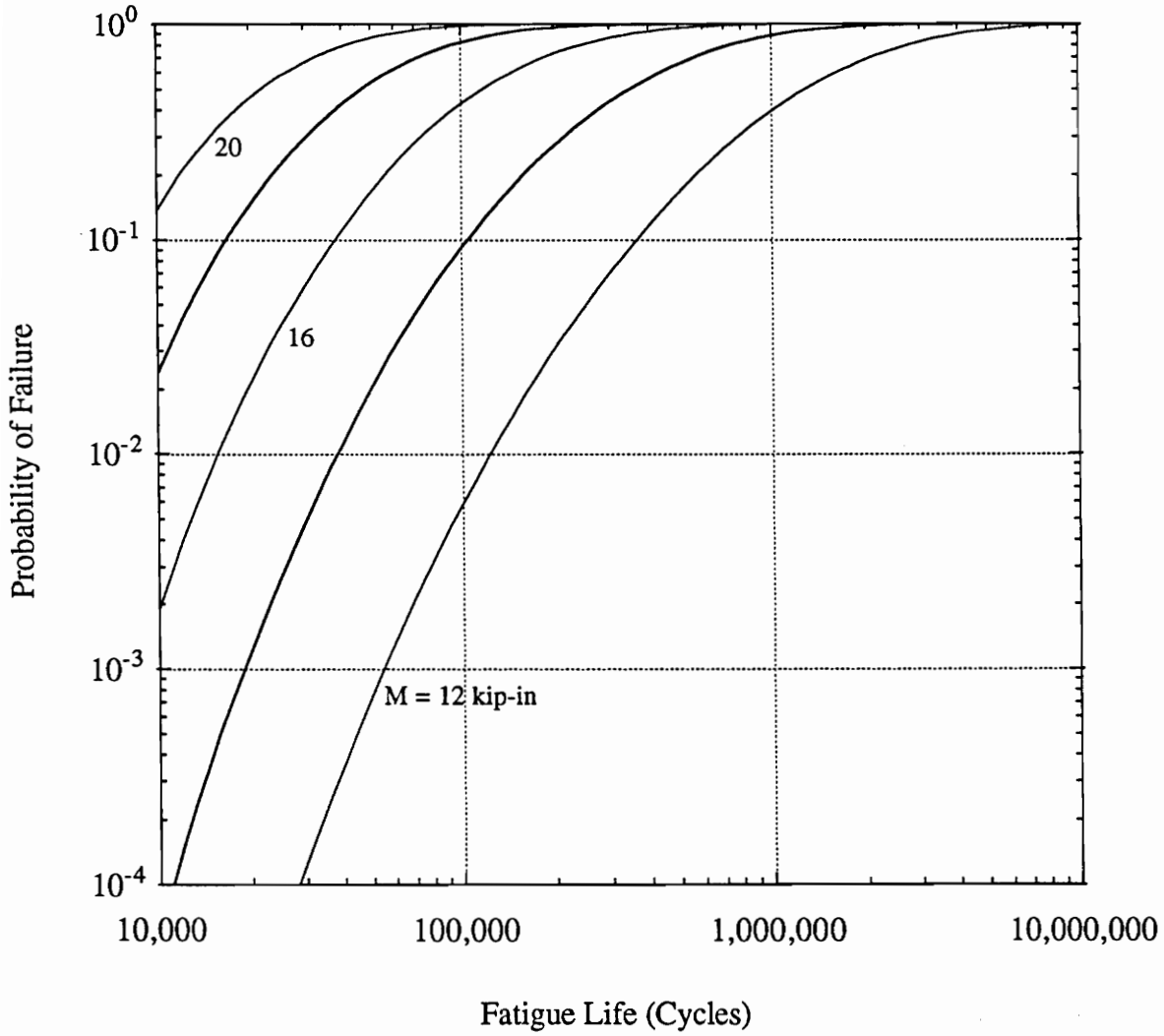

Figure 8c : P_f vs. Cycles for Aluminum 5454

Driver Variations

The second stage of examination involved assessing variations in driving habits and how they affect wheel performance. This so-called human element is a significant factor in determining the number and degree of maximum stresses developing over the service history of many vehicle components, but accurately measuring these different driving habits remains a formidable task. One approach taken by Audi engineers involved using a vehicle equipped with strain gages mounted on the wheel hub and sending 25 customers over a single 64-mile route representative of average German driving conditions [14]. Audi also employed a professional test driver to traverse the same route for comparison purposes. The recorded load peak distributions were converted to equivalent lateral acceleration values, which could then be related to a rotational bending moment by analyzing the mechanics of the vehicle. These moment spectra were normalized to the test driver's data, which was taken as the most severe (100% full scale). From this spectra, a table of cycle counts at various percentiles of the maximum moment was developed, and is shown in Table 2. In addition to the driver spectra, data from a similar test performed by LBF Laboratory is also included for comparison (the numbers are higher due only to a much longer test run). This data was incorporated into the second reliability program and used to compute a failure probability by a method based on total probability theory.

Essentially, total probability theory describes the probability of an event (e.g. Q) occurring in terms of its intersection with any number of mutually exclusive and collectively exhaustive events, E_n [1]. Mathematically,

$$P[Q] = \sum_i P[Q|E_i] \cdot P[E_i] \tag{3.1}$$

where $P[Q|E_i]$ is translated as *the probability of Q occurring given that event E_i has already occurred.* In this case, the P_f can be determined by considering the P_f of the wheel assembly at a specified percent full-scale moment and the probability of this magnitude of moment occurring. Since

Table 2: Audi Wheel Spectra

Moment	*Cycle Count per Driver*					
(% FS)	*Test*	*1%*	*3%*	*50%*	*97%*	*LBF*
100%	3					80
95	17					520
90	35					900
85	55	2				2000
80	60	5	2			4500
75	50	13	4			8000
70	100	15	9			14,000
65	50	35	20			25,000
60	100	50	35	3		40,000
55	100	80	80	12		55,000
50	200	100	150	35	2	80,000
45	150	200	200	70	6	140,000
40	300	300	300	180	22	330,000
35	800	400	400	400	120	700,000
30	2000	800	800	1300	450	1.6×10^6
25	6000	4000	4000	2000	1400	4.0×10^6
20	10,000	9000	9000	11,000	6000	1.3×10^7
15	15,000	15,000	15,000	15,000	17,000	4.0×10^7
10	20,000	25,000	25,000	25,000	30,000	4.0×10^7
Total	55,020	55,000	55,000	55,000	55,000	1.0×10^8
Miles	64.6					186,000

the probability of any specified moment occurring for each percentile driver is given by the ratio of the number of observed cycles at that moment level divided by the driver's total cycle count, the P_f can then be calculated from

$$P_{f,driver} = P_f|(M = 100\%) \cdot \frac{(cycles@M = 100\%)}{\sum cycles} + P_f|(M = 95\%) \cdots \quad (3.2)$$

This equation is represented by line 60 in the second program listed in the Appendix.

The magnitude of moment taken as 100% full scale was calculated by considering the 1900 ft·lb fatigue test from [9], and dividing out the scaling factor of 1.6. Converting units to kip·inches, the full-scale moment was found to be around 14.5. Maximum lateral acceleration values given in [4], when converted to moments, confirmed this to be a reasonable estimate of the maximum service load developed in the wheel.

Results from the analysis of driver spectra are shown in Figure 9. Here, again, the curves for 1010 steel and 5454 aluminum are very similar, with a 1% driver producing a failure probability of about one in 100 at 200,000 miles with 1010 steel and seven in 1000 with aluminum. An average driver gave a P_f of three in 1000 and two in 1000, respectively, for the 1010 steel and aluminum at a similar mileage. The dual phase steel yielded much lower failure curves (note the different y-axis scale); a 1% driver could expect one failure in 1000 at 200,000 miles, whereas a 50-th percentile driver might expect only three chance wheel failures out of 100,000 after the same period with dual phase. This is typical of the kind of information — both qualitative and quantitative — that could be derived from these results, which should prove of interest to design, quality assurance, and safety engineers.

Route Variations

Another way of categorizing wheel stress variations is by examining the routes and surfaces over which a vehicle traverses. An in-depth study performed by the Motor Industry Research Association investigated the effects

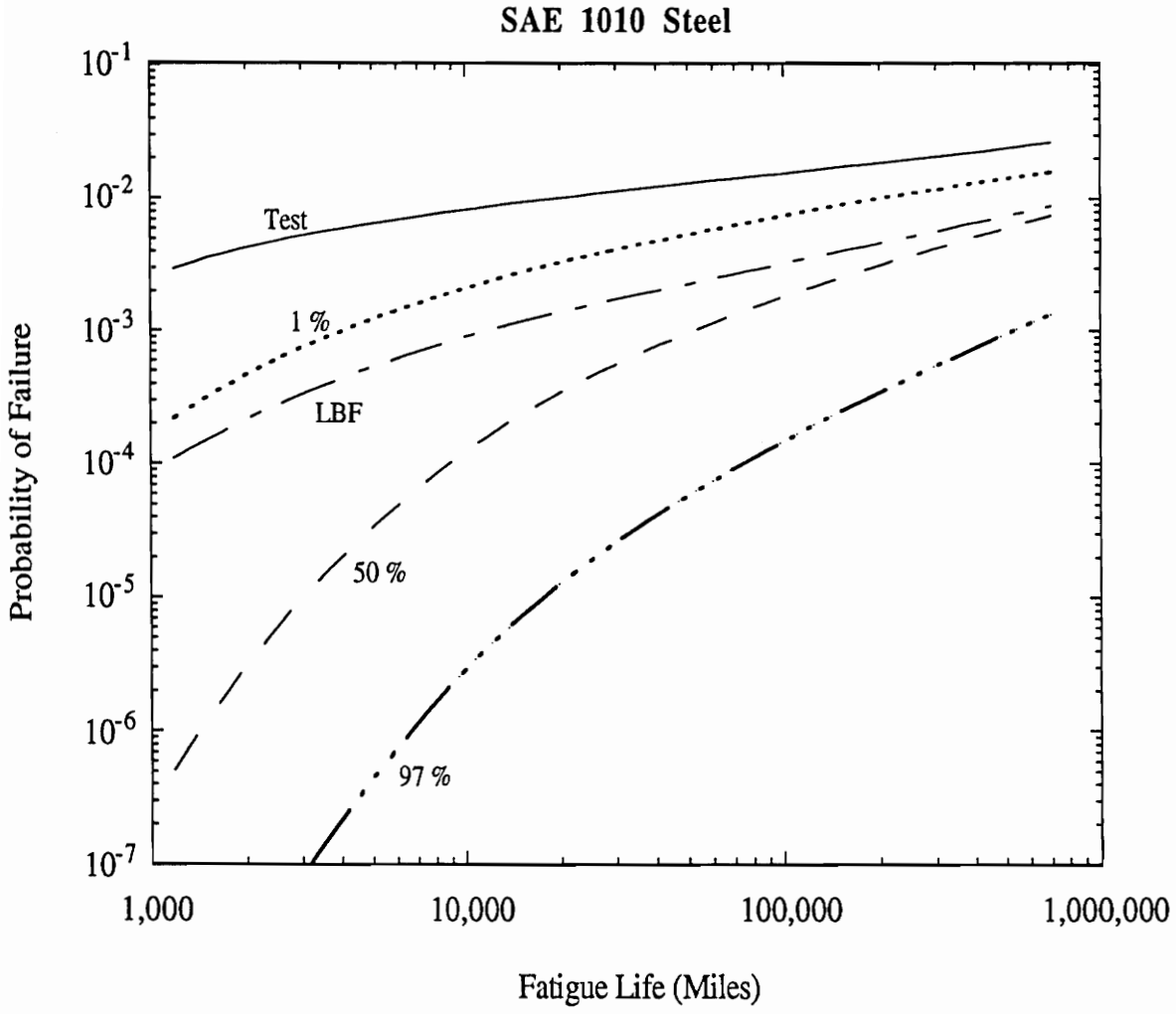

Figure 9a : P_f vs. Miles for Percentile Drivers (SAE 1010)

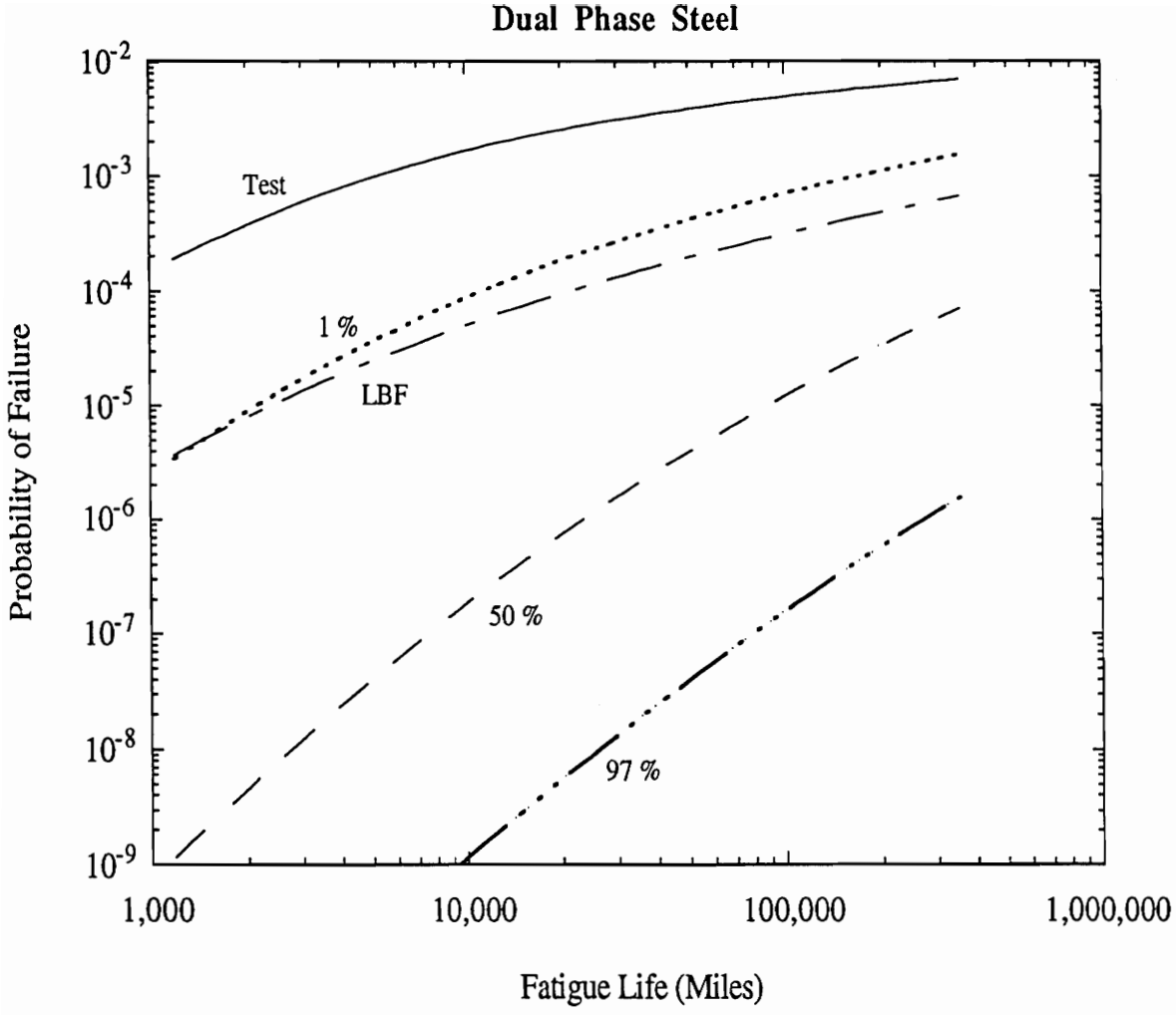

Figure 9b : P_f vs. Miles for Percentile Drivers (Dual Phase)

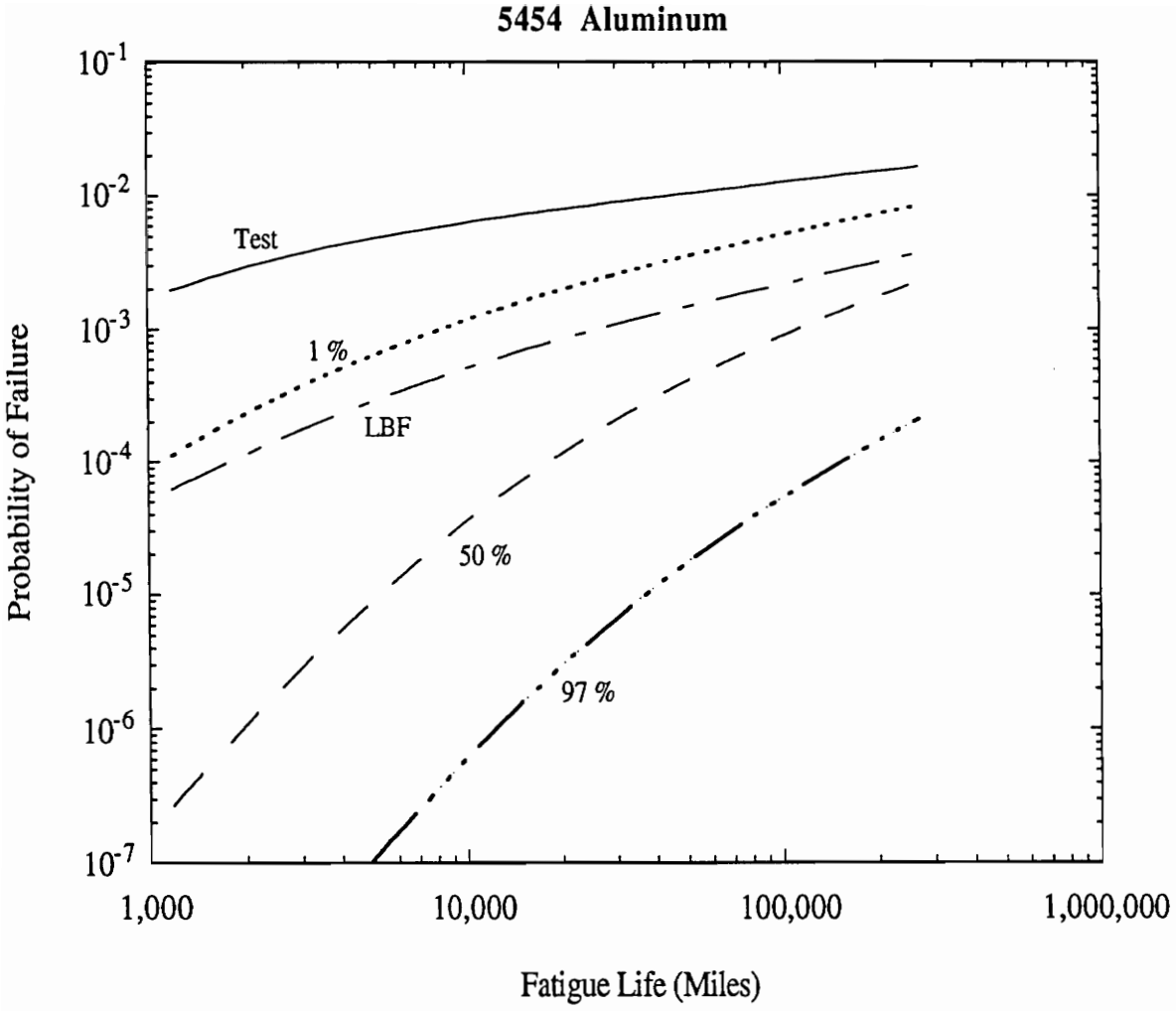

Figure 9c : P_f vs. Miles for Percentile Drivers (Al 5454)

road surfaces and steep, crooked roads had on wheel performance [4]. The eight routes chosen for this case study were split into British and Continental segments, the latter being located in the Alps of Southern France. Brief descriptions of each route are as follows:

London :	from North London into and around the city center (18 miles)
Derbyshire II :	rural route in a hilly district with moderately severe corners (54 miles)
Leicester :	classified rural roads (49 miles)
A5 :	main highways in rural areas (59 miles)
Col de Turini :	main continental route containing severe corners and gradients (38 miles)
Col de Braus :	similar to Turini, but with less severe corners and gradients (32 miles)
Col de Bleine :	corners and gradients similar to Braus, but with loose road surfaces (44 miles)

A distribution of cycle counts for each route was formulated based on percentages of total wheel revolutions at a specified moment [4]; this data was normalized to the largest moment observed, and is summarized in Table 3. An analysis similar to that of the driver spectra was performed, again utilizing total probability concepts. A maximum moment of 14.5 kip·inch — hereafter used as the 100% full scale moment — was also used in processing the failure curves shown in Figures 10 and 11. As expected, the Alpine routes with the sharpest corners and steepest gradients produced the highest P_f of the continental roads, and the side roads and city driving gave the highest P_f for the British routes. Again the dual phase steel outperformed the remarkably similar 1010 and aluminum wheels by a considerable margin. Two significant observations were made from these results. First of all, even though Col de Turini was the worst continental road chosen, the slow driver here actually developed the lowest failure curve of all the other Alpine routes, further emphasizing the influence of driving habits on fatigue

Table 3: MIRA Wheel Spectra

Moment (% FS)	*Continental*				*British*			
	Turini Fast	*Turini Slow*	*Col de Braus*	*Col de Bleine*	*London*	*Derby Part II*	*Leicester*	*A5*
100%	146		21		8	5		
85	54		305	8	17	80	62	9
69	1172	51	633	225	46	299	46	66
54	3534	368	1054	784	54	912	196	180
38	3005	1540	935	1861	152	2414	899	180
23	3790	3292	2416	3921	281	4524	2789	657
8	4933	4690	3465	6713	5482	16,888	23,014	10,345
Total	31,665	31,687	26,035	37,524	15,351	46,780	41,624	49,420
Miles	*38*		*32*	*44*	*18*	*54*	*49*	*59*

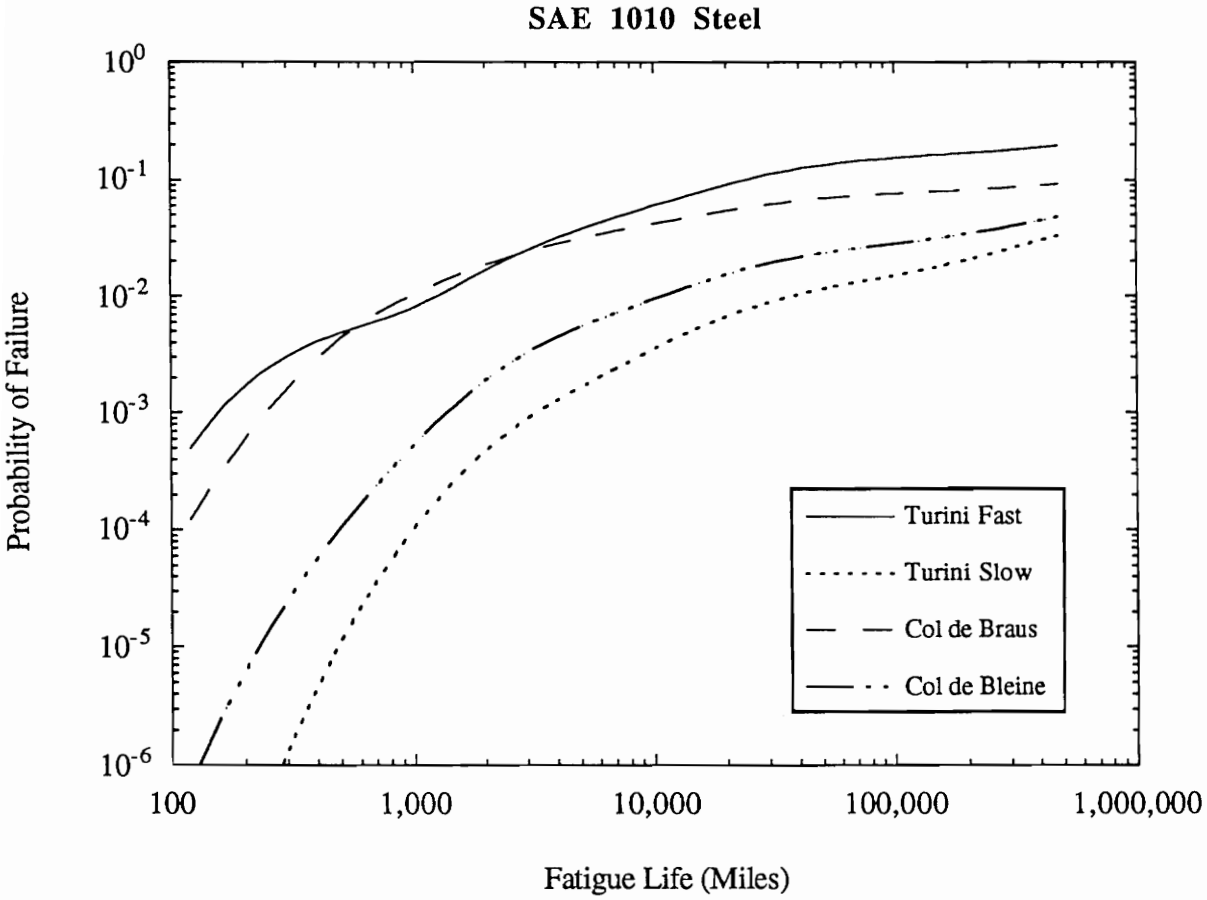

Figure 10a: P_f vs. Miles for Continental Routes (SAE 1010)

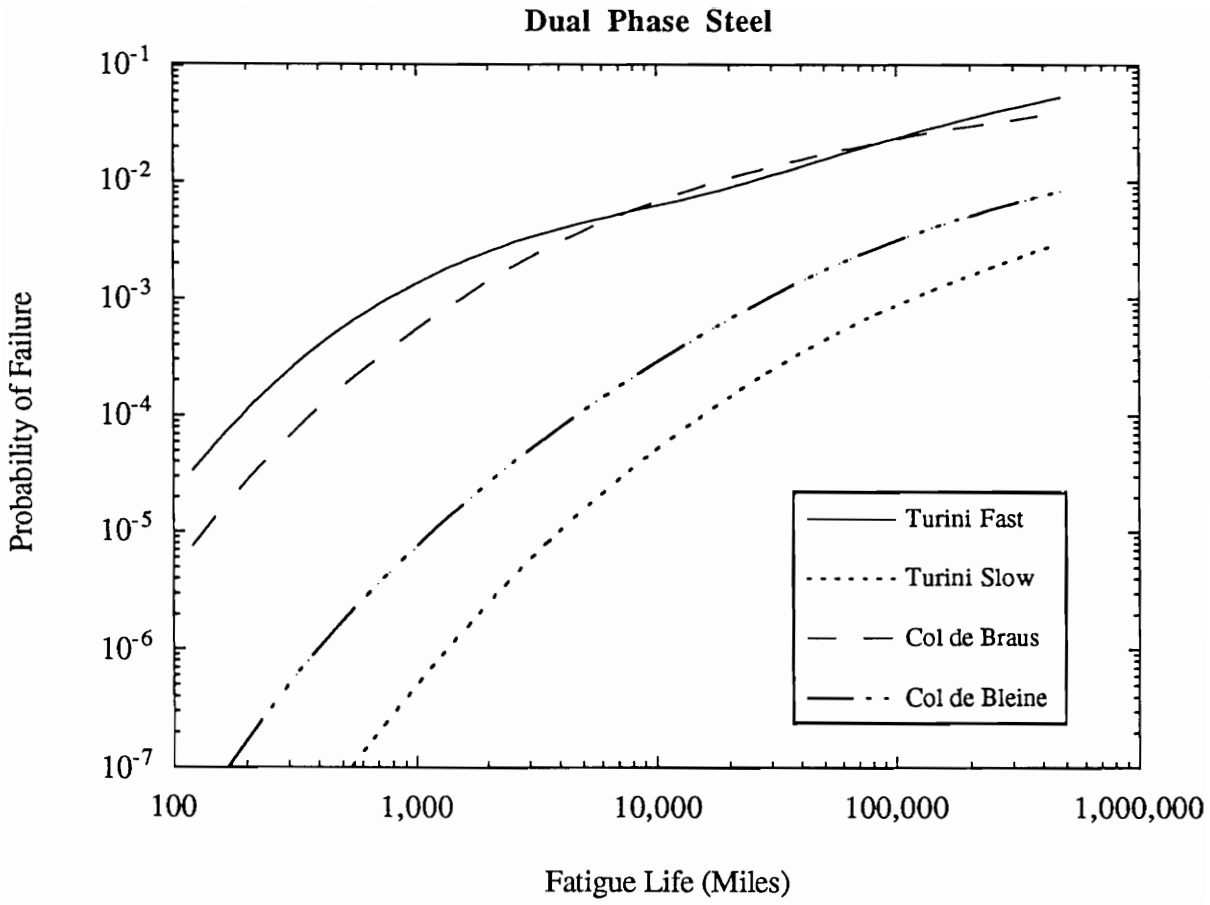

Figure 10b : P_f vs. Miles for Continental Routes (Dual Phase)

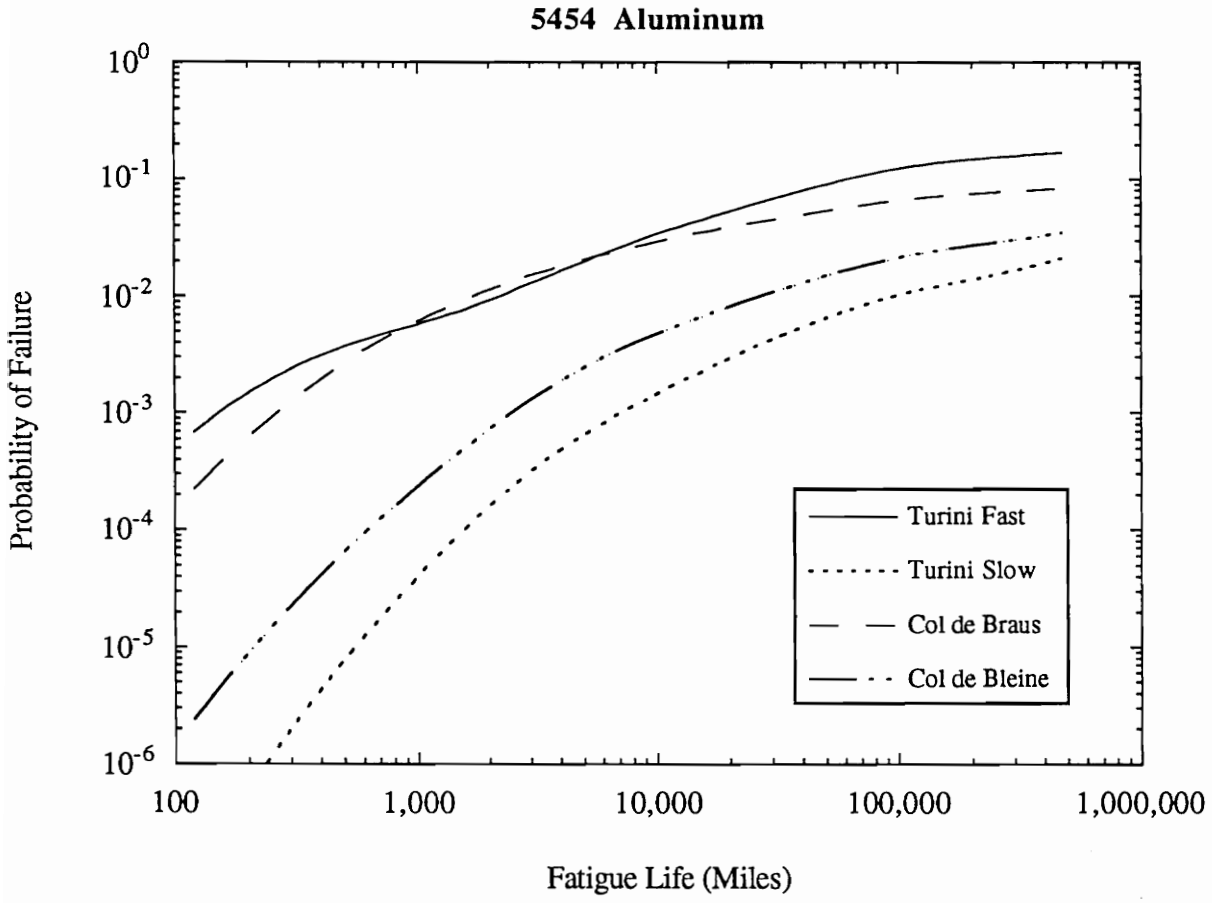

Figure 10c : P_f vs. Miles for Continental Routes (5454 Al)

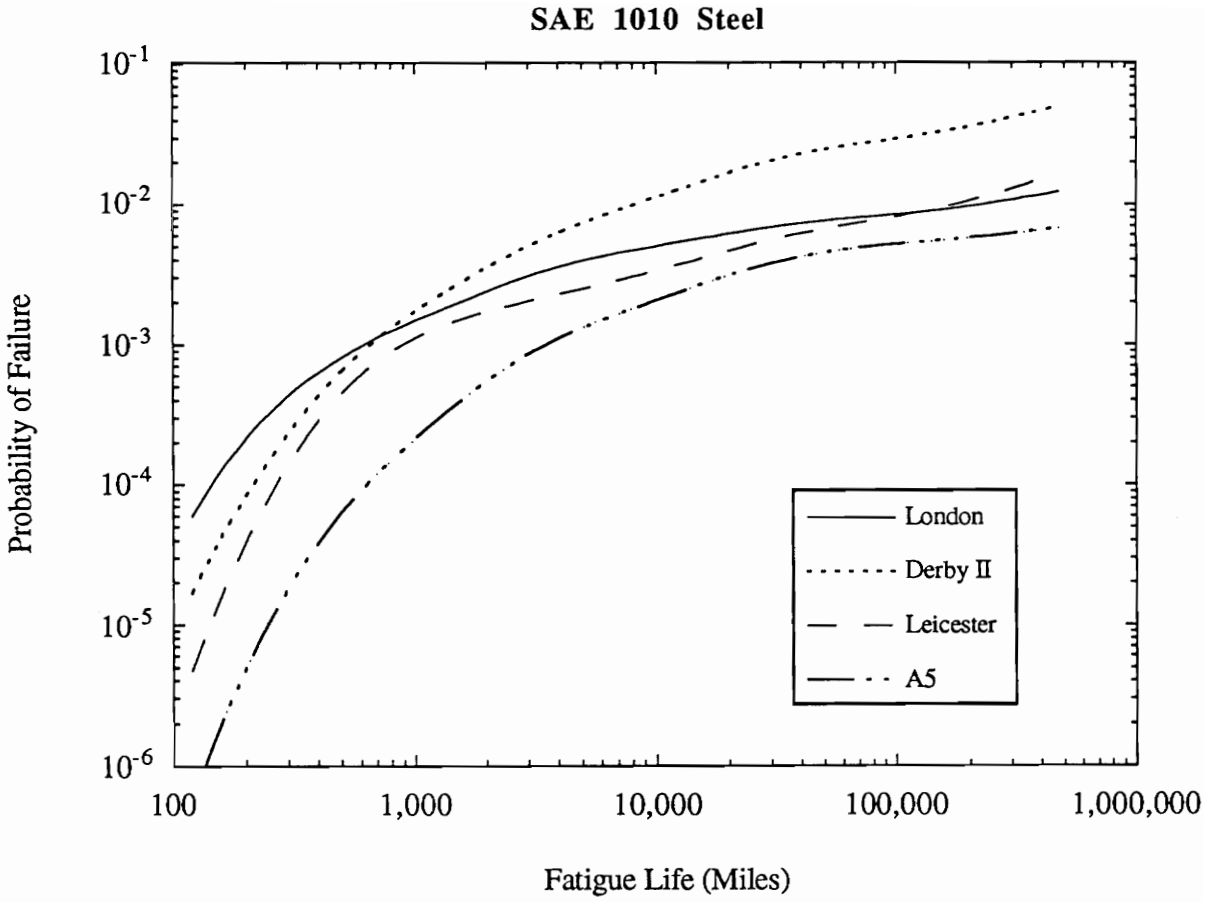

Figure 11a : P_f vs. Miles for British Routes (SAE 1010)

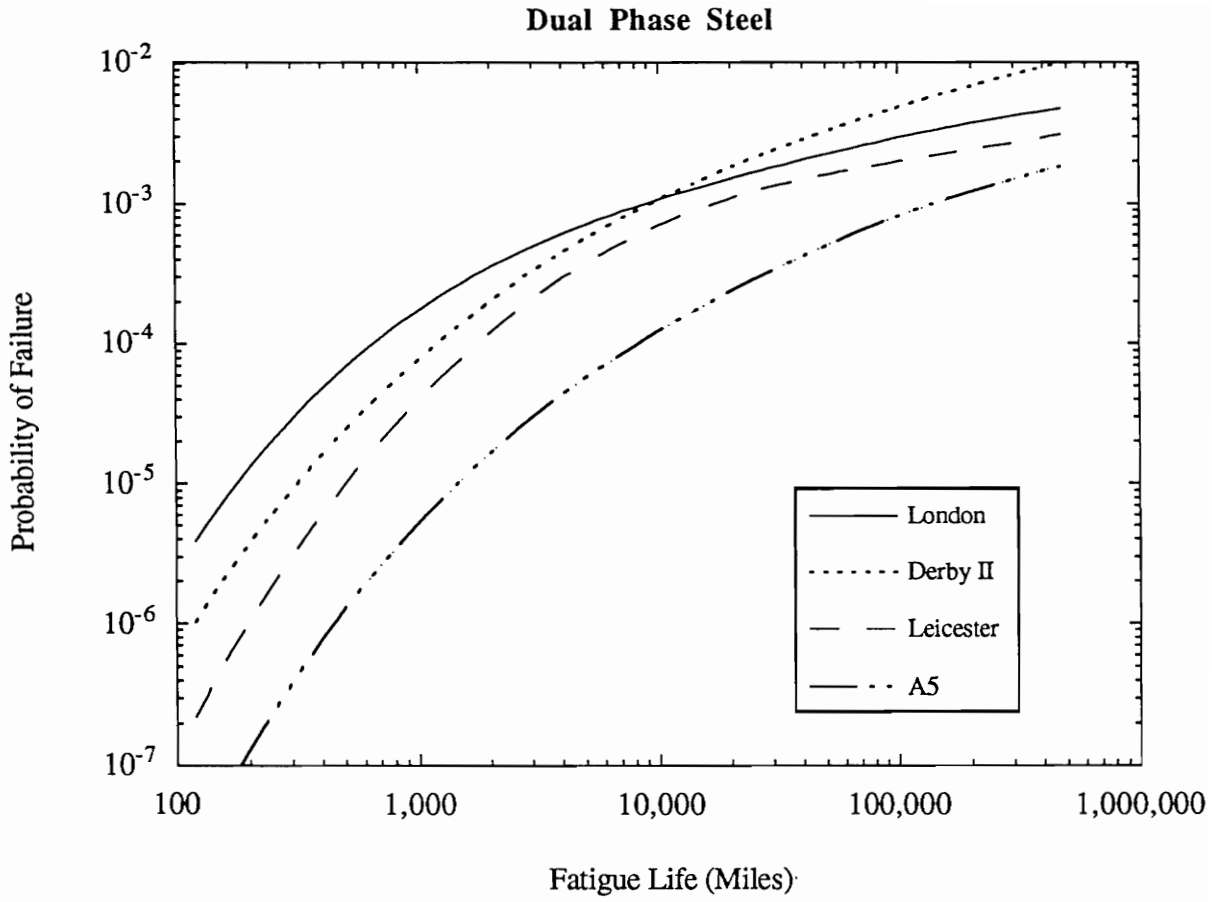

Figure 11b : P_f vs. Miles for British Routes (Dual Phase)

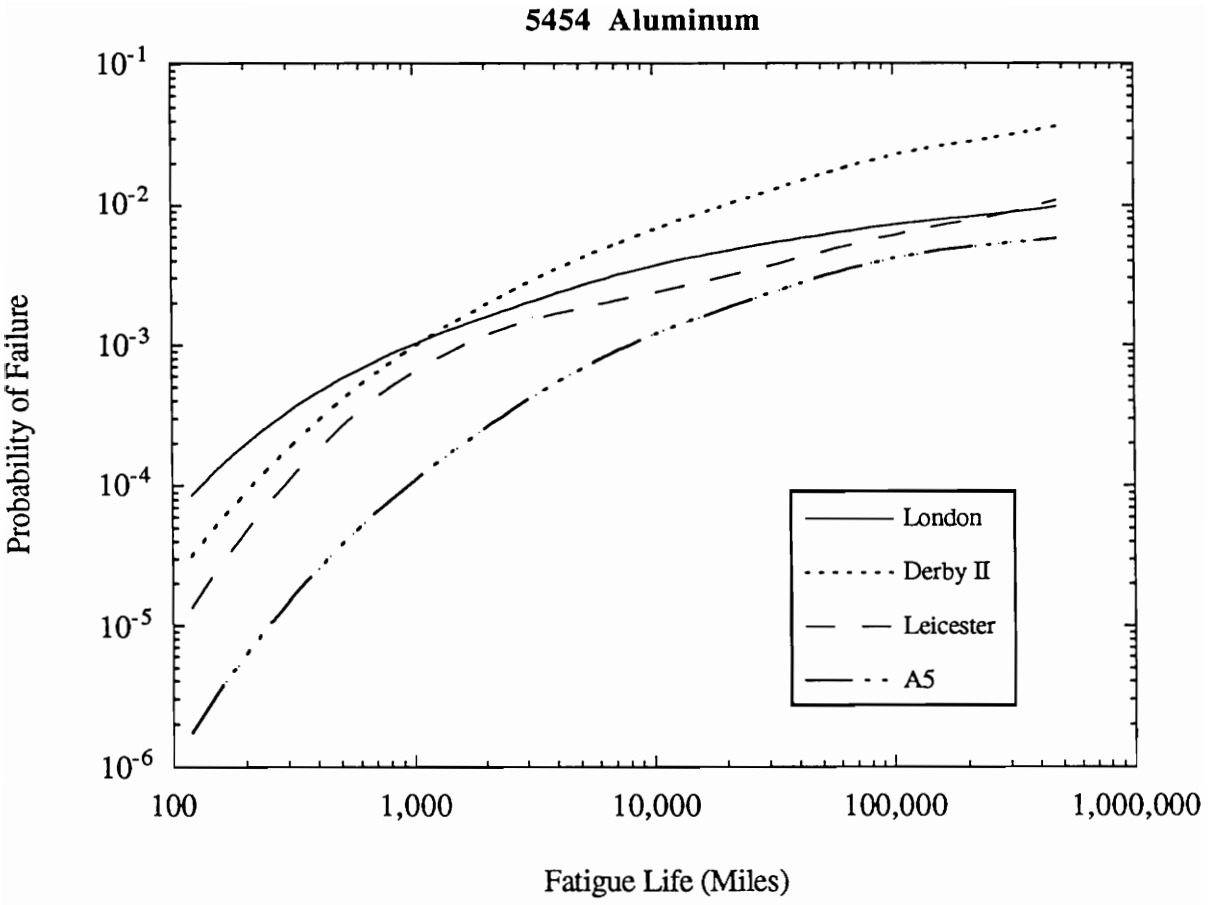

Figure 11c : P_f vs. Miles for British Routes (5454 Al)

life. The dip in the Turini Fast curve — which occurred in all three materials tested — remains somewhat of a mystery, but is most likely linked to the skewed cycle count distribution. Another key observation from the British route results stemmed from the crossover of the London and Derbyshire curves. Interestingly enough, at lifetimes under 1000 miles (10,000 for dual phase), city driving actually produced the most wheel damage, even though the Derbyshire route was categorized as being the most severe of the English routes.

The results illustrate well the effect of route (and driver) variations on the fatigue life of wheel assemblies. However, from a design engineer's perspective it would be quite impractical to design a wheel assembly around failure curves such as this, since no driver would accumulate such high mileages from a single exclusive road type. A better method is to apportion the various routes into representative fractions of total service life, and then synthesize these "partial routes" into a characteristic mileage history.

Route Synthesis

Integration of the various test routes into a realistic service history entailed normalizing the roads to a standard mileage and multiplying each route's cycle count by the fraction of total service life it was to represent. In this case, the road lengths were all normalized to 100 miles, with the cycle counts (from Table 3) being increased accordingly. It was then necessary to break down the routes into percentages typical of common usage environments. All four British routes were included in this route synthesis, as well as the continental Col de Braus; the latter was chosen on the basis of the failure curves of Figure 10 as being the best representative of a mountainous route. Three such combined routes were developed: an "average" route, composed of 40% freeway, 30% highway, 15% city, 10% rural, and 5% mountainous routes; a "traveling" type route, with a respective breakdown of 60, 20, 15, 5, and 0%; and a "lŏcal" route, composed of 10% freeway, 20%

highway, 35% city, 20% rural, and 15% mountain roads. It should be noted that nothing more than simple logic was involved in determining these ratios, but for reference, Wimmer portrayed an average route as being composed of 20% freeway, 48% highway, and 32% urban routes [14]. The results of this exercise are shown in Figure 12.

In choosing local and traveler route distributions it was possible to establish upper and lower bounds on the failure curves for each plot. Once again, the dual phase wheel gave a reliability considerably higher than either other alloy — about three failures in 1000 at 100,000 miles for an average route, compared to roughly one in 100 for both HRLC steel and aluminum. While one failure in 100 at only 100,000 miles sounds alarmingly high for any strategic vehicle component, it is to be emphasized that a failure here designates only the cycles (or miles) required to initiate a crack. Also, material processing effects have not yet been considered; this is the topic of the following exercise.

Material Processing Effects

All of the former tests have dealt with variations in the stresses applied to a wheel assembly and their effect on wheel performance. These stress variations directly affected the value of S in the limit-state equation, thus changing the overall reliability. However, the forming process also has a pronounced impact on service life, as it may alter certain material properties used to determine fatigue life. In this case, the strength R changes the system reliability (refer to the flow chart in Figure 6). The most obvious change due to processing occurs in the fatigue strength exponent, b; with cold working (CW) most materials see an improvement in fatigue life, and the value of b will decrease according to a slightly flatter elastic strain-life line. Table 1 gives material properties for all three alloys subjected to 20% cold working (the exponent b is estimated for dual phase). These properties were applied to the previous route synthesis algorithm, so that a quantitative comparison

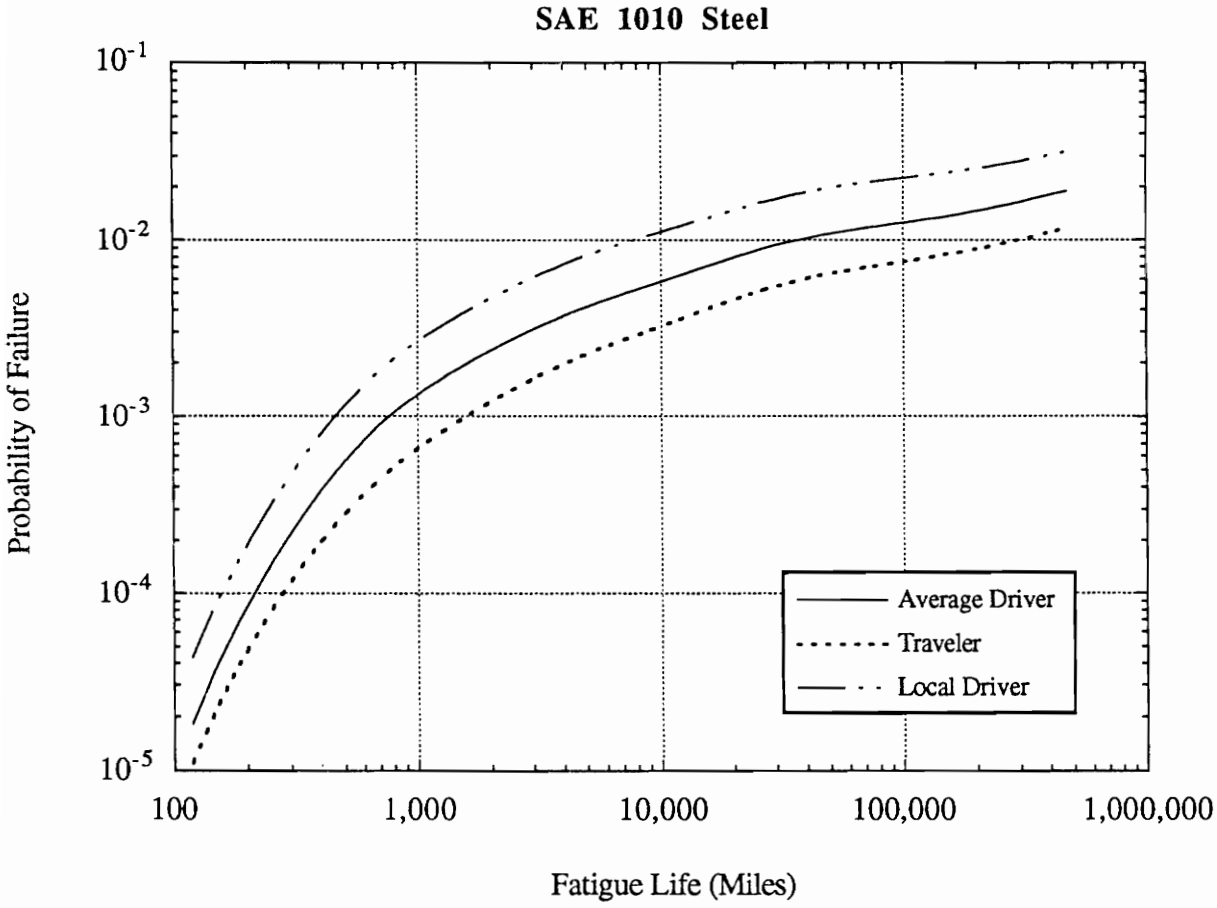

Figure 12a: P_f vs. Miles for Synthesized Routes (SAE 1010)

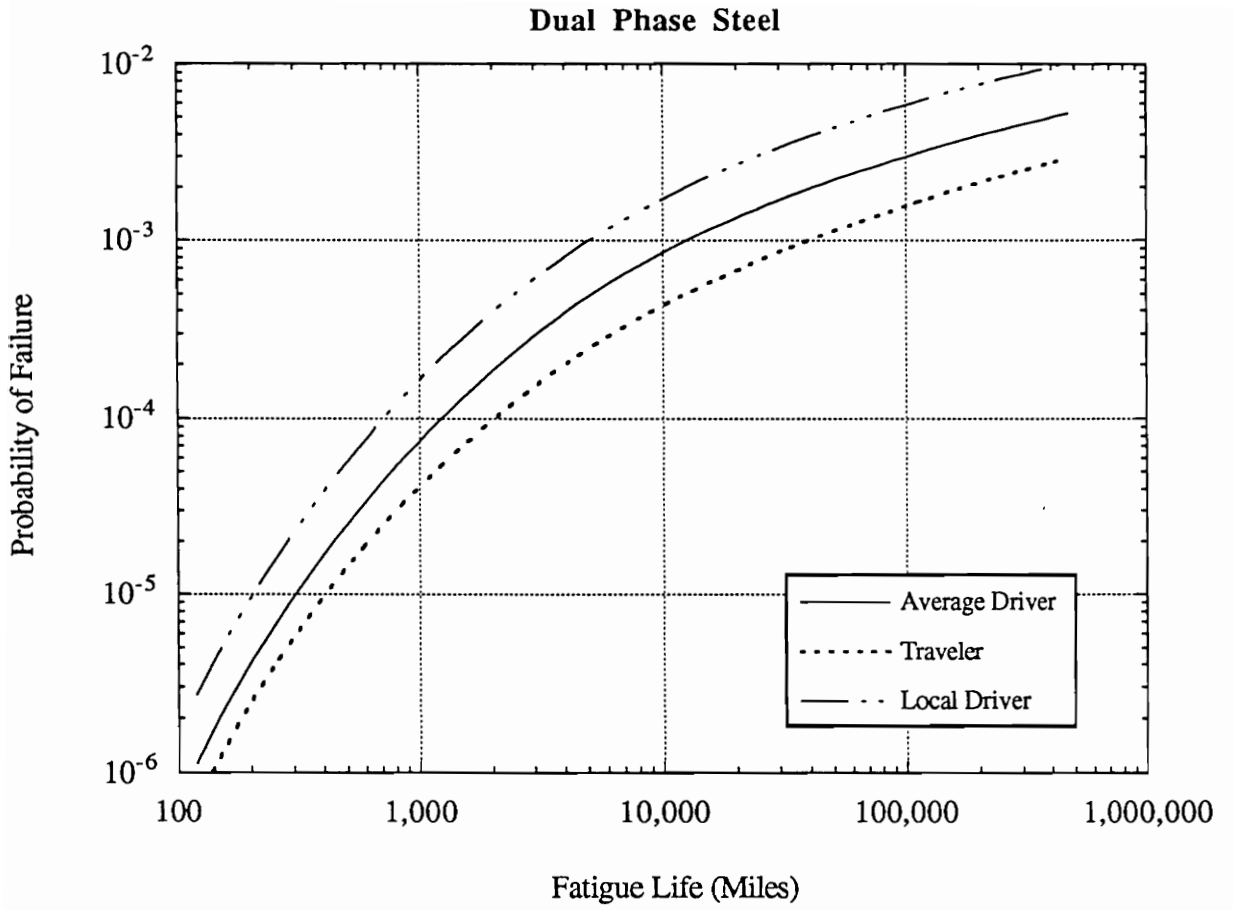

Figure 12b : P_f vs. Miles for Synthesized Routes (Dual Phase)

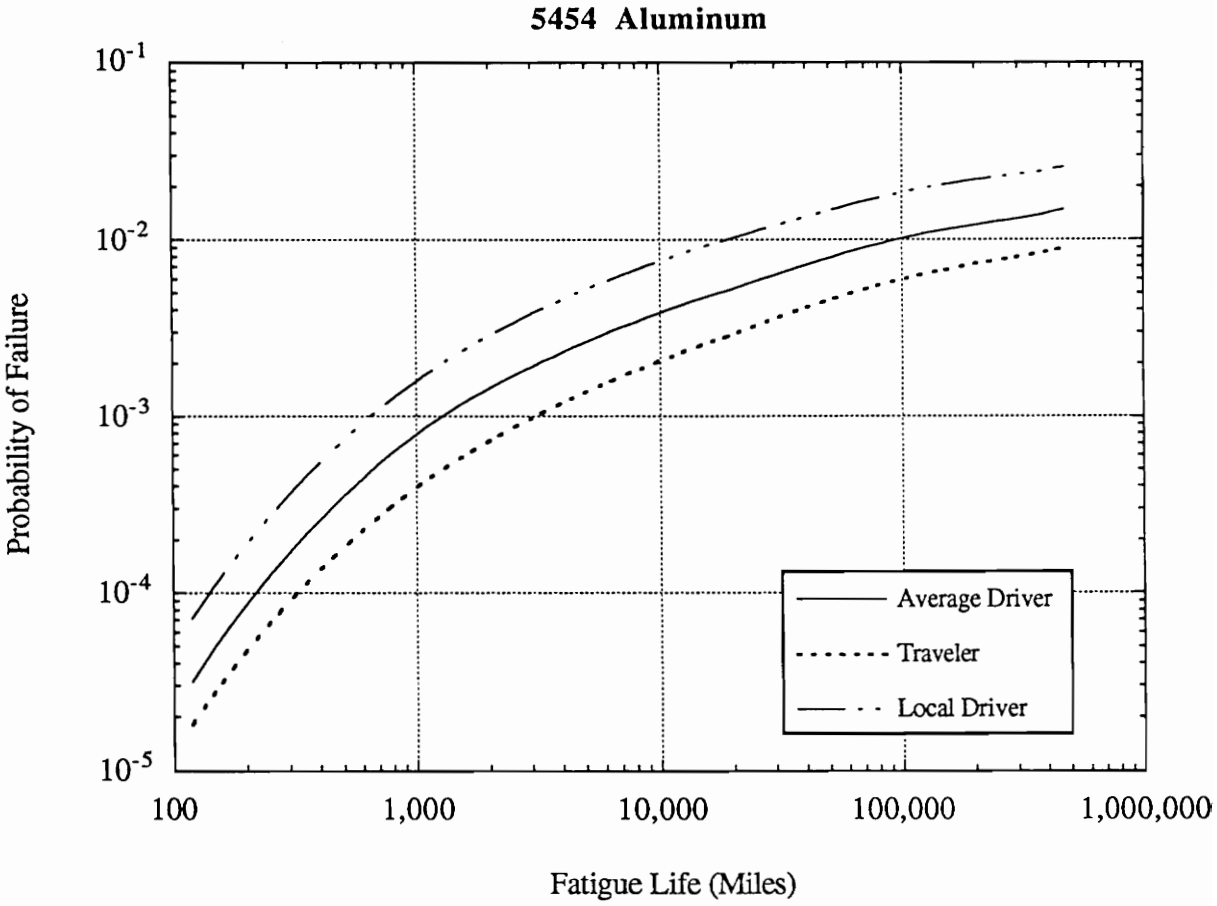

Figure 12c : P_f vs. Miles for Synthesized Routes (5454 Al)

of fatigue lives could be made.

Figure 13 illustrates the effect of cold working by showing a substantial reduction in each failure curve (compare to Figure 12). An average route that produced about one failure in 100 at 100,000 miles using 1010 steel would now yield only three chance failures in 1000. Due to a more modest CW effect, the difference in the aluminum wheel reliability was slightly less pronounced. However, an assumed reduction in the fatigue strength exponent for dual phase steel produced a remarkable improvement in failure rates (note the shifted y-axis). A wheel subjected to cold working and driven on an average 100,000–mile route might experience only 35 chance failures in a million, whereas DP steel as-received may yield three in 1000 — or almost 100 times more — failures. Obviously the effects of cold working are not to be ignored.

The single biggest factor influencing fatigue life, then, is the fatigue strength exponent, b, an observation shared by [5]. Further processing may cause the fatigue intercepts or the ductility exponent to fluctuate in either direction, but since the total strain-life line approaches the elastic line at long lives, the slope of this elastic line becomes paramount in fatigue life calculations.

Choice of Distributions

As previously discussed, the use of normally distributed random variables is in itself an approximation of the actual distributions. Types of distributions are numerous, and practically any shape dispersion can be modeled by a mathematical formula. Since data was not available in most cases, a normal distribution was taken as a reasonable estimate of each variable's actual dispersion; however, an improper assumption of distribution type can affect the system reliability just as a bad dispersion value can.

In further analyzing the wheel assembly, the 5454 aluminum (CW) material properties and thickness were modeled as log normal random variables with similar dispersions, and the reliability was calculated for the synthesized

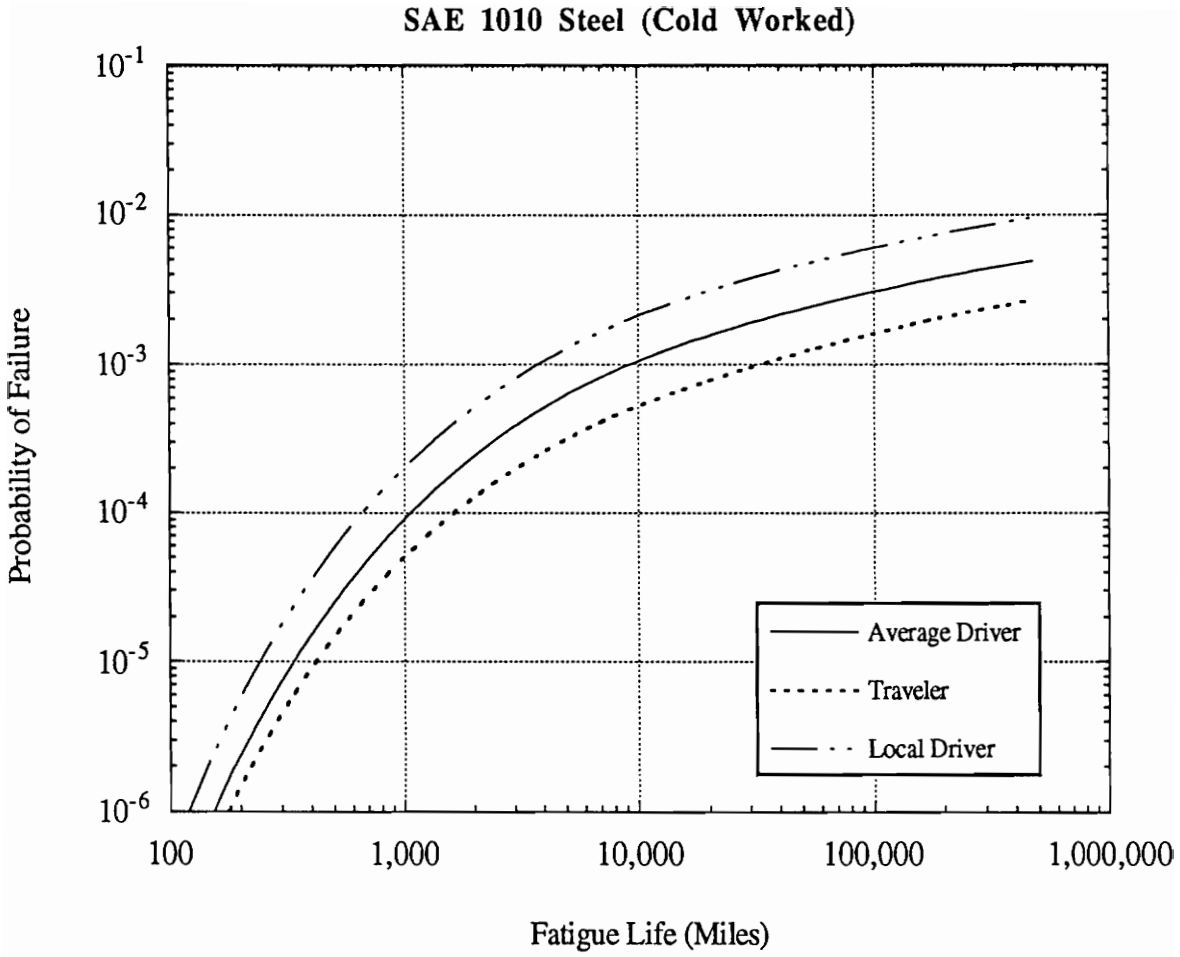

Figure 13a : P_f vs. Miles for Synthesized Routes (SAE 1010, CW)

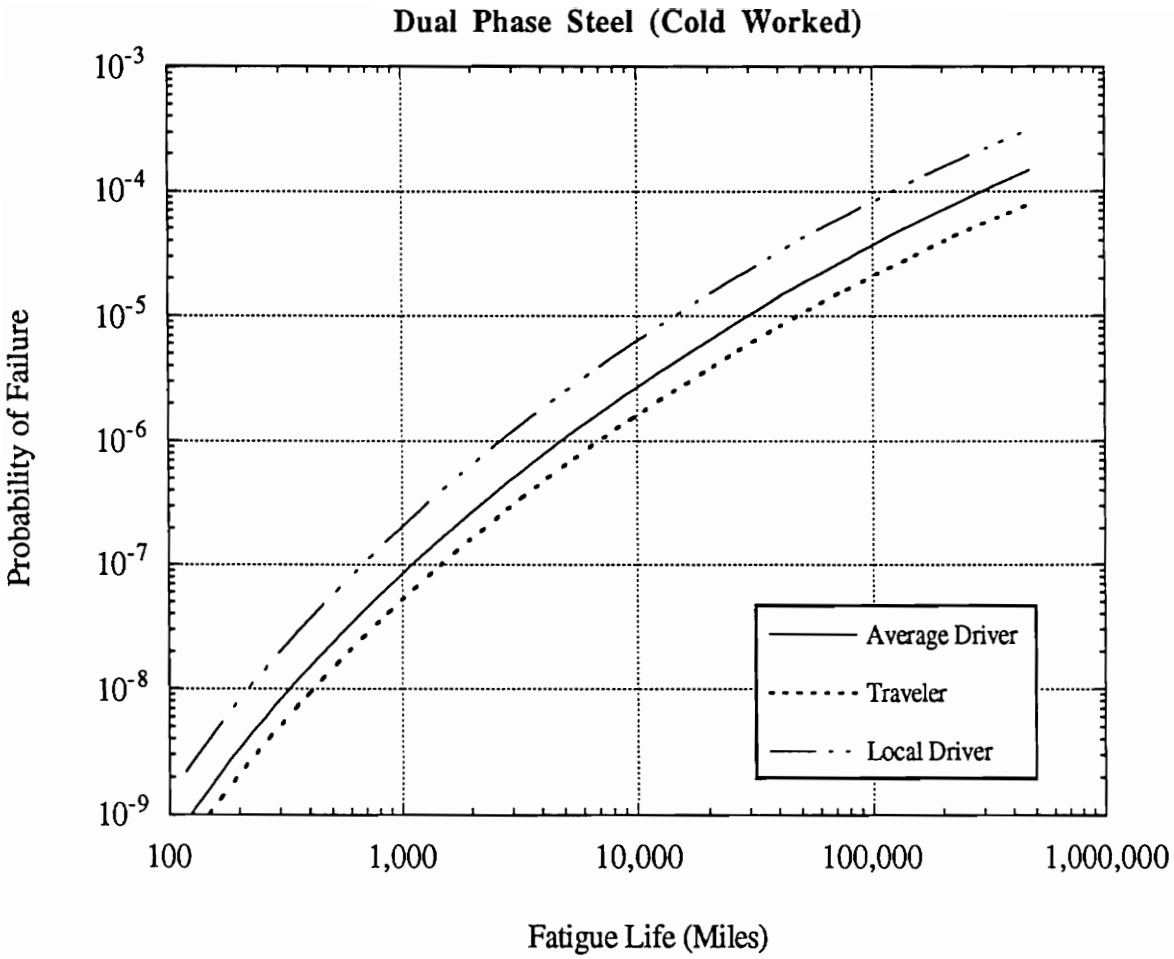

Figure 13b : P_f vs. Miles for Synthesized Routes (Dual Phase, CW)

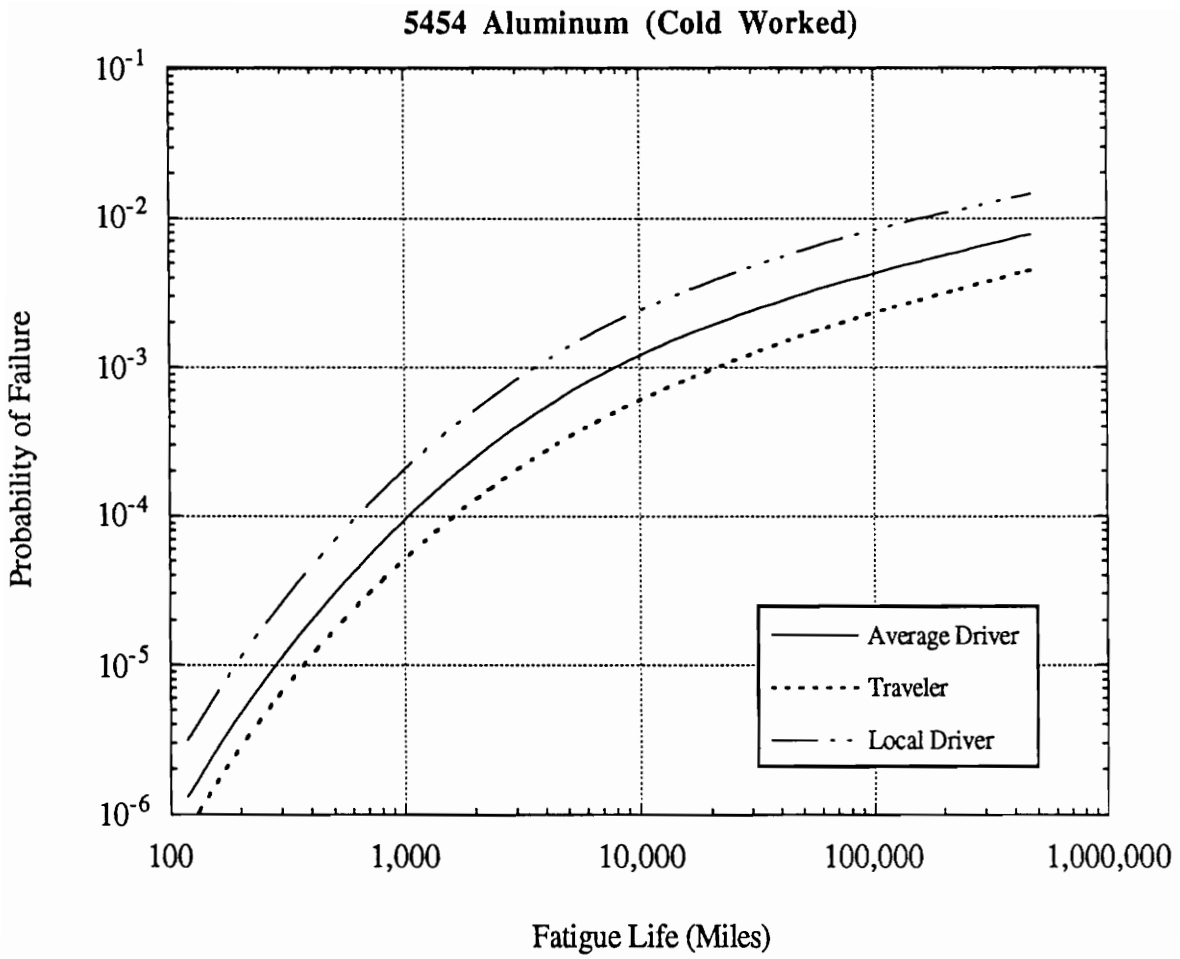

Figure 13c : P_f vs. Miles for Synthesized Routes (5454 Al, CW)

routes. A comparison of the average driver's results indicated that — in this case — the choice of normal or log normal distributions made little difference, as the change in system reliability at long lives was negligible. At 100,000 miles, the P_f for each route decreased by only two in 10,000 (this value was ascertained from the output data, since the curves in Figure 14 were essentially identical past 1,000 miles). The similarity of these failure curves shows only that normal and log normal distributions describe the random variables equally — it says nothing of *how well* they describe this set of parameters. To ultimately choose the best distribution requires either prior knowledge of that specific distribution, or, ideally, a reasonably large set of data with which to establish via probability calculations the best fit distribution.

As a final investigation of wheel performance, the random variable distributions were again manipulated — this time only by changing the magnitude of dispersion — in an attempt to convey a possible solution for designers working to increase a system's reliability. Using normally distributed variables, the thickness standard deviation was reduced to one-fourth of its original value. Results of this test were marginal, as the change in P_f was slight at high mileages. Ideally, a comparison could be made between results from the given dispersions and those of quasi-deterministic random variables, so that the information obtained might serve to increase design efficiency. Thus, if controlling a particular variable is fairly expensive or time-consuming, this type of analysis would identify up front the benefits of tighter tolerances, and the feasibility of better controlling these parameters could then be quickly assessed.

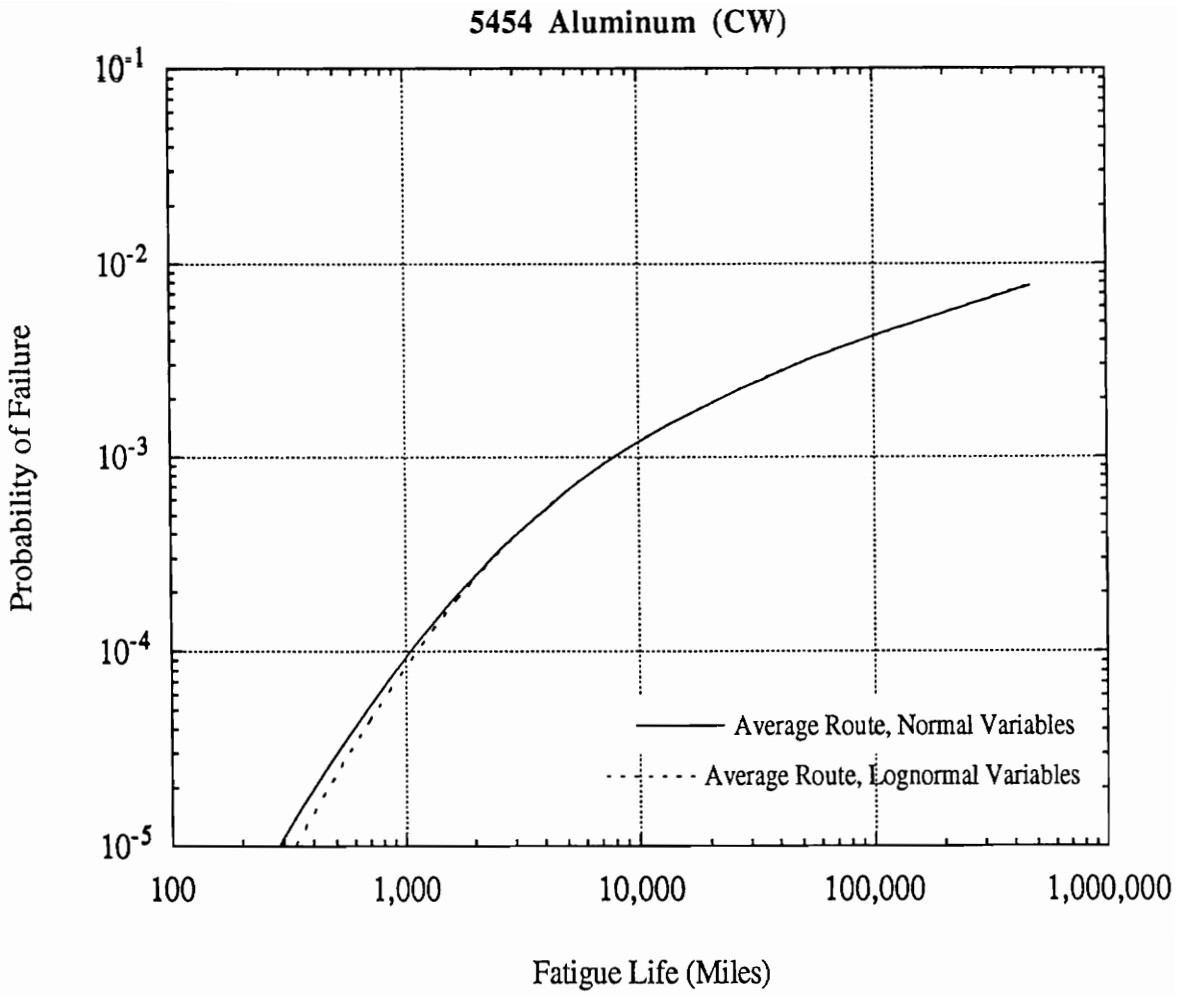

Figure 14 : Comparison of Distributions for Synthesized Routes (5454 Al)

SUMMARY AND CONCLUDING REMARKS

In summarizing the information collected throughout the various stages of analysis, the final synthesized-route graph utilizing cold worked material properties was used as a general guideline for determining overall component reliability. It is clear that dual phase steel would produce the most reliable wheel spider of the three alloys chosen, based not only on this last graph, but on the results at every stage of the analysis. For comparison purposes, Germany requires its wheels to cover 186,000 miles of average driving routes with a failure probability of not more than 10^{-5} [14]. As can be seen from the average route curve for DP steel (Figure 12b), the P_f is slightly higher than 10^{-5}, reading about 6×10^{-5} at 186,000 miles. However, it should be emphasized that the "average" mileage breakdown here includes mountainous and rural routes (which are the most damaging), whereas the German definition of an average route is limited to highway and urban driving. Obviously this basic difference in definition would skew these failure curves towards the high side, so given similar loading conditions the numbers would probably compare quite well.

Even with cold working effects included, the results for 1010 steel and 5454 aluminum do not correlate with either the dual phase performance or the German requirements. A chance failure rate of four in 1,000 for an average road mileage of 100,000 would be totally unacceptable by modern standards, the only consolation being the fact that this represents mileage to crack initiation only. If these materials were fairly resistant to crack growth, then this value could in actuality be quite adequate.

This case study emphasized only component reliability in determining the best material for the job. However, several other factors ultimately need to be considered before a final decision can be made. Included among these are the benefits of weight reduction, material and production costs, and material formability. The failure curves used to assess component reliability could also be utilized to identify problems associated with *over*-design (e.g.

a spider thickness greater than necessary would yield a very low P_f, and result in material waste and excessive weight); therefore, this analysis package would also prove useful in portraying the economical impact of material downgaging. Economics will always play a large role in the reduction and substitution of materials used in mass-produced components, so even though durability/reliability may arguably be the most important factor to consider, it is but one of many steps involved in product design and optimization. By investigating the diverse loading histories and property variations characteristic of this real-world problem, though, a more accurate and detailed portrayal of the wheel spider's actual service performance can be used in making better decisions regarding material substitution and subsequent design improvements.

In analyzing the automobile wheel assembly, an example was made of the type of engineering problem that could be confronted with the durability/reliability design package developed here. By collecting information regarding the geometry, loading, and distribution of design variables in any given problem, however, this analysis could easily be applied to again predict component service performance. Thus, in no way is this application limited to ground vehicle design; instead, it offers a variety of designers an efficient alternative to the age-old design-test-redesign routine.

Future Study

As this exercise represented an initial union of durability and reliability methods, there exist several opportunities for improvement. From the durability standpoint, the following areas need attention before the full scope of this type of analysis can be realized:

Improved data acquisition and storage techniques, to allow for more diverse and thorough component testing;

More accessible (on-line) material property databases, which will permit much easier material substitution;

A strictly deterministic damage algorithm such as Palmgren-Miner, which will enable direct comparison of this new procedure with results from "standard" methods;

The implementation of a crack growth algorithm employing plane stress fracture mechanics concepts, in order to handle crack propagation lifetimes.

The probabilistic algorithm utilized in this case study would benefit from the introduction of these additional parameters:

The use of correlated random variables, to better model the interdependence of material properties;

An algorithm to choose the best-fit distribution and dispersion from available raw data, which will eliminate any guesswork regarding distributions and increase the accuracy of the results;

In this specific case, the inclusion of b (fatigue strength exponent) as a random variable, due to the critical nature of this material property in determining fatigue life.

The implementation of these additional concepts will ultimately enhance the accuracy and flexibility of this type of analysis, making it a much more practical design tool.

APPENDIX : RELIABILITY PROGRAMS

```
c     Program RELIAB1 employs subroutine FNBETA() and function GFNTN()
c     to compute the probability of failure of a wheel spider
c
      PARAMETER (NVMX=6,NTMX=9)
      IMPLICIT DOUBLE PRECISION (A-H,O-Z)
      DIMENSION AMOMT(10),RCYCL(200),PROBF(200,10)
      DIMENSION CRMTX(NVMX,NVMX),WKMTX(NTMX,NTMX)
      DIMENSION AMEAN(NVMX),ASTDV(NVMX),WKVTR(NVMX),IDTN(NVMX)
      EXTERNAL GFNTN
      COMMON/BLOCK1/RMOMT,RLIFE,B,C
      DATA IWRT/0/
c
c     fatigue strength and ductility exponents (deterministic)
c     (SAE 1010 shown)
c
      B = -0.096D0
      C = -0.440D0+B
      B = 2.D0*B
      READ(5,*) NVAR,NCOR
c
c     input type of distribution, mean, stdv for each variable
c
      DO 10 IV=1,NVAR
   10 READ(5,*) IDTN(IV),AMEAN(IV),ASTDV(IV)
c
c     determine vectors of moments and cycle counts
c
      NMNTS = 5
      DO 20 KK = 1, NMNTS
   20 AMOMT(KK) = 12.D0 + DBLE(KK-1)*2.D0
      RE = 7.D0
      RI = 4.D0
      NPTS = 76
      DR = (RE-RI)/DBLE(NPTS-1)
      DO 30 NN = 1, NPTS
   30 RCYCL(NN) = 1.D1**(RI+DBLE(NN-1)*DR)
c
c     begin iterative loop
c
      DO 40 II = 1, NMNTS
      RMOMT = AMOMT(II)
      DO 40 JJ = 1, NPTS
      RLIFE = 2.D0*RCYCL(JJ)
   40 CALL FNBETA(GFNTN,NVAR,IDTN,AMEAN,ASTDV,ABETA,PROBF(JJ,II),
     :IWRT,NCOR,CRMTX,NVMX,WKVTR,WKMTX,NTMX)
      DO 50 II = 1,NPTS
   50 WRITE (6,100) RCYCL(II),(PROBF(II,NN),NN=1,NMNTS)
  100 FORMAT (10(1X,E9.3:))
      END
```

```
c     function GFNTN(*) computes R, S, and returns G=R-S
c
      FUNCTION GFNTN(VECT)
      IMPLICIT DOUBLE PRECISION (A-H,O-Z)
      DIMENSION VECT(*)
      COMMON/BLOCK1/RMOMT,RLIFE,B,C
c
c     compute strength
c
      RVBLE = DSQRT(VECT(3)*VECT(3)*(RLIFE**B)
     $ + VECT(2)*VECT(3)*VECT(4)*(RLIFE**C))
c
c     compute stress
c
      SVBLE = 0.153D0*RMOMT*(VECT(1)**(-1.4D0))
c
      GFNTN = RVBLE - SVBLE
      RETURN
      END
```

```
c     Program RELIAB2 takes data regarding moment distributions
c     for various drivers and computes a Pf for each
c
      PARAMETER (NVMX=6,NTMX=9)
      IMPLICIT DOUBLE PRECISION (A-H,O-Z)
      DIMENSION AMOMT(9),RCYCL(200),PFTOT(200,10)
      DIMENSION VAL(30,10),SUM(10)
      DIMENSION CRMTX(NVMX,NVMX),WKMTX(NTMX,NTMX)
      DIMENSION AMEAN(NVMX),ASTDV(NVMX),WKVTR(NVMX),IDTN(NVMX)
      EXTERNAL GFNTN
      COMMON/BLOCK1/RMOMT,RLIFE,B,C
      DATA IWRT/0/
      DO 5 L=1,10
      DO 5 M=1,200
 5    PFTOT(M,L)=0.D0
      B = -0.0868D0
      C = -0.5856D0+B
      B = 2.D0*B
      READ(5,*) NVAR,NCOR
      DO 10 IV=1,NVAR
 10   READ(5,*) IDTN(IV),AMEAN(IV),ASTDV(IV)
      NMNTS = 1
      DO 20 KK = 1, NMNTS
 20   AMOMT(KK) = 14.5D0 + DBLE(KK-1)*3.D0
      RE = 9.0D0
      RI = 6.0D0
      NPTS = 76
      DR = (RE-RI)/DBLE(NPTS-1)
      DO 30 NN = 1, NPTS
 30   RCYCL(NN) = 1.D1**(RI+DBLE(NN-1)*DR)
c
c     enter sum of cycle counts for each driver
c
      READ(5,*) (SUM(NN),NN=2,6)
c
c     read value of % moment and number of cycles at that moment
c
      DO 35 JJ=1,19
 35   READ(5,*) (VAL(JJ,KK),KK=1,6)
c
c     begin iteration
c
      DO 80 II = 1, NPTS
        RLIFE = 2.D0*RCYCL(II)
        DO 60 KK=2,6
        DO 60 JJ=1,19
c
          RMOMT = AMOMT(1)*VAL(JJ,1)
c
          CALL FNBETA(GFNTN,NVAR,IDTN,AMEAN,ASTDV,ABETA,PROBF,
     :    IWRT,NCOR,CRMTX,NVMX,WKVTR,WKMTX,NTMX)
```

```
c
c      sum Pf's for each driver at each cycle count
c
 60   PFTOT(II,KK) = PFTOT(II,KK) + PROBF*VAL(JJ,KK)/SUM(KK)
c
      RCYCL(II) = RCYCL(II)/851.D0
  80  WRITE (6,100) RCYCL(II),(PFTOT(II,KK),KK=2,6)
 100 FORMAT (E9.4E1,1X,7(1X,E9.4E2:))
      STOP
      END
      FUNCTION GFNTN(VECT)
      IMPLICIT DOUBLE PRECISION (A-H,O-Z)
      DIMENSION VECT(*)
      COMMON/BLOCK1/RMOMT,RLIFE,B,C
      RVBLE = DSQRT(VECT(3)*VECT(3)*(RLIFE**B)
     $ + VECT(2)*VECT(3)*VECT(4)*(RLIFE**C))
      SVBLE = 0.153D0*RMOMT*(VECT(1)**(-1.4D0))
      GFNTN = RVBLE - SVBLE
      RETURN
      END
```

REFERENCES

1. Ang, A. H-S., and Tang, W.H., Probability Concepts in Engineering Planning and Design, Volume I: Basic Concepts, John Wiley, New York, 1975.

2. Ang, A. H-S., and Tang, W.H., Probability Concepts in Engineering Planning and Design, Volume II: Decision, Risk, and Reliability, John Wiley, New York, 1990.

3. Bannantine, J., Comer, J., and Handrock, J., Fundamentals of Metal Fatigue Analysis, New Jersey, Prentice-Hall, Inc., 1990.

4. Bingham, D.C.H., and Crane, C., "Road Wheel Stresses," Warwickshire, UK, Motor Industry Research Association, 1977.

5. Boardman, Bruce, "Crack Initiation Fatigue–Data, Analysis, Trends, and Estimation," Warrendale, PA, Society of Automotive Engineers, Paper #820682, 1982.

6. Conle, F.A., Landgraf, R.W., and Richards, F.D., Ford Materials Databook: Monotonic and Cyclic Properties of Engineering Alloys, Ford Motor Company, 1984.

7. Dowling, N.E., Mechanical Behavior of Materials, N.E. Dowling, 1989 (to be published).

8. Grubisic, V., and Lowac, H., "Possibility to Determine Aluminum Wheels Fatigue Life by Local Strain Concept," Warrendale, PA, Society of Automotive Engineers, Paper #880696, 1988.

9. Landgraf, R.W., "Fairmont/Zephyr Wheel Downgaging," Ford Motor Company, 1980.

10. Landgraf, R.W., and Conle, F.A., "Vehicle Durability Analysis," Concurrent Engineering of Mechanical Systems, New York, American Society of Mechanical Engineers, 1990.

11. Makin, P.C., et al., "Development of Steels for Automobile Wheels," Australia, Broken Hill Proprietary Co., Ltd., 1982.

12. Thangjitham, S., and Landgraf, R.W., "Probability–Based Methods for Fatigue Analysis," Warrendale, PA, Society of Automotive Engineers, Paper #920661, 1992.

13. Vinogradov, Oleg, Introduction to Mechanical Reliability: A Designer's Approach, New York, Hemisphere Publishing Corp., 1991.

14. Wimmer, A., and Peterson, J., "Road Stress Resistance and Lightweight Construction of Automobile Road Wheels," Warrendale, PA, Society of Automotive Engineers, Paper #790713, 1979.

VITA

Richard Lee Ridder was born in Ohio in December of 1967 and raised in Western Maryland, where he graduated from high school in 1986. He then entered Bridgewater College in Bridgewater, Virginia, to pursue a degree in the physical science field. He completed his undergraduate work at Bridgewater in the spring of 1990 and graduated magna cum laude with a Bachelor of Science degree in Physics. In the fall of 1990 he entered the Department of Engineering Science and Mechanics at Virginia Polytechnic Institute and State University, and completed a Master of Engineering degree in August of 1992. His career plans involve engineering applications in the areas of structural analysis, fracture mechanics, and reliability. Hobbies include volleyball, tennis, music, and model trains.